Aggregation Behavior of Keratin Proteins Determined by Dynamic Light Scattering

Alexandra Marie Egert

Thesis submitted to the faculty of the Virginia Polytechnic Institute and State University
in partial fulfillment of the requirements for the degree of

Master of Science
In
Materials Science and Engineering

Mark E. Van Dyke, Chair
E. Johan Foster
Richey M. Davis

April 24, 2015
Blacksburg, VA

Keywords: Keratin, Dynamic Light Scattering, Aggregation, Buffer

Aggregation Behavior of Keratin Proteins Determined by Dynamic Light Scattering

Alexandra Marie Egert

ABSTRACT

Keratin is a biomaterial derived from biological sources and can be used in a variety of medical applications. This study focuses on keratin derived from human hair. Unfortunately, there is not a lot of information in the literature describing how keratin reacts to subtle changes in an aqueous solution such as differences in pH, keratin concentration, buffer concentration, salt concentration, and temperature. To have a better understanding of this effect, dynamic light scattering was used to test the size ranges and volume percentages in each range. Dynamic light scattering shows the size of the keratin in each environment and its consistency with time. The results showed that there is a difference in keratin behavior between water and buffer solutions, but very subtle differences between each buffer, buffer concentration, keratin concentration, pH and temperature. Keratins aggregate extensively in un-buffered conditions (i.e. pure water), which has implications to both purification and fabrication of biomaterials as water is used extensively in these processes. Interestingly, there was little effect of keratin concentration, pH, and temperature on the buffers used in this study, suggesting there may be a wide range of conditions in which aggregation can be minimized.

Acknowledgements

I would like to thank the Dean's Office in the Virginia Tech College of Engineering for funding support through the Incentive Graduate Assistantship Program.

My biggest thanks goes to my advisor, Dr. Van Dyke, for all the support, conversation, and time he has given me. I am very grateful that he accepted me to be one of his first graduate students here at Virginia Tech. He has taught me almost everything I know about research, and he has taught me life lessons through the many tangents in lab meeting.

I would also like to thank my committee, Dr. Davis and Dr. Foster for their support throughout my research. I would especially like to thank Dr. Davis for the many hours he spent with me discussing the data.

I would like to thank the members of my lab, Michele Waters, Alexis Trent, Jamelle Simmons, Roche DeGuzman, and Maria Rahmany for their constant help and support.

I would like to thank the undergraduates, Cornelius Leary III, Rachel Ladenburger, and Brian Odenwald, for the many hours they spent working on lab work.

I would also like to thank Steve McCartney for help with the scanning electron microscopy, Caleb King for the statistics help, and Ami Jo for help with dynamic light scattering.

Finally, I would like to thank my parents and my fiancé, Ian Clark, for their constant love and support. I would not be where I am today without their belief in me.

Thank you everyone!

Alexandra Egert

Table of Contents

List of Figures

List of Tables

CHAPTER 1 -INTRODUCTION

1.1 MOTIVATION

The majority of medical devices and implants that go inside the human body are made from materials that are foreign to the human body, such as metals, ceramics, and artificial polymers. The human body will not recognize these types of materials and will respond to them in various ways, sometimes causing serious medical complications. If a medical device is made from a material designed to be either inert or favorably interact with the body, often referred to as a biomaterial, then there is less of a chance that the body will reject it. Materials derived or inspired by nature are an important class of biomaterials. Proteins and carbohydrates make up the largest classes of naturally-derived biomaterials, and among these several structural proteins such as collagen have been extensively studied and used in clinical practice. Another structural protein, keratin, has much less widely studied and there are almost no current clinical uses. However, it has been shown in multiple studies that keratin biomaterials are compatible with cells and tissues, and can form the basis of medical devices and other biomedical technologies [1]. Unfortunately, much of the published literature surrounding keratin biomaterials describes this material in terms of the methods used to produce it rather than its actual composition and inherent characteristics. Keratin biomaterials are typically produced by chemically treating keratin-containing tissues (e.g. hair, hooves, feathers, etc.) to render the proteins soluble, extracting, and purifying various preparations of the resulting proteins and reaction by-products. There are multiple methods of extracting keratins which will be described later. These varied methods lead to different compositions that result in keratin biomaterials with different material properties, making much of the resulting published observations

dependent on the preparation method, rather than the inherent properties of keratin. If an extraction and purification process directed toward isolation of the constituent protein (or protein complex) can be realized, meaningful structure-property relationship studies can be undertaken. For this goal to be realized, an understanding of the solution behavior of extracted keratin must be developed and applied to the extraction process itself, as well as the process of forming biomaterial structures (e.g. hydrogels) from purified keratins. For this goal to be realized, a better understanding of how the solution affects the behavior of extracted keratin must be developed and applied to the extraction process itself, as well as the process of forming biomaterial structures (e.g. hydrogels) from purified keratins. Testing parameters such as salt, buffer, pH, temperature, and keratin concentration against a control as well as comparing the parameters to each other will help explain how the keratins behave in different environments, particularly with regard to aggregation behavior. Aggregation, or more importantly control of aggregation behavior, is one of the most important aspects of keratin purification and the formation of keratin-based biomaterials.

1.2 INTRODUCTION TO KERATINS

Keratins are a family of structural proteins found in mammals such as humans, whales, sheep, and cows, and which are located in body parts such as skin, hair, nail, baleen, wool, and horns. Because of the different functions of these body parts, keratins can be split up into two types: hard and soft. Hard keratins are found in hair and nails, while soft keratins are found in skin [2].

Marshall et al. show that hair keratins, the focus of the current study, have high levels of glutamic acid, half-cystine, and glycine, but very low levels of histidine,

methionine, and phenylalanine [2]. Keratins, formerly called cytokeratins, are coded by fifty-four different genes. The genes can be split up into type 1 and type 2. Type 1 keratins are acidic while type 2 keratins are basic to neutral. Type 1 hair keratins can be labeled as Ha1-Ha8 (H for hair and A for acidic), or as K31-K40. Type 2 hair keratins can be labeled as Hb1-Hb6 (H for hair and B for basic), or as K81 to K86. There are thirty-seven epithelial keratins and seventeen hair keratins. There are seventeen type 1 epithelial keratins and twenty type 2 epithelial keratins, while there are eleven type 1 hair keratins and six type 2 hair keratins [3]. Only hair keratins were used in this work and will be the focus of further discussions.

Intermediate filaments (IF) are formed from certain structural proteins and are typically found in the cytoplasm of cells. Some common IF are, vimentin, neurofilament, lamins, desmin, and keratin [4]. Crewther et al. did a study on keratin IF and showed that the basic coiled-coil structure is similar to other IF such as desmin and vimentin. The building blocks of IF are polymerized forms of the protein. In the case of keratin (as well as most other IF-forming proteins), there are helical coil regions of the proteins that interact, as well as head and tail regions that serve to stabilize polymerization. The coiled regions are the same throughout the keratin family, but the head and tail regions are non-deterministic structures that lead to heterogeneity. Dimerization of two keratin proteins, as well as further coordination of dimers, is fairly well understood, but assembly of higher ordered structures as well as complete formation of IF has not been determined, although a few theoretical models exist. Differences in head and tail regions make it difficult to determine the absolute size of a keratin dimer. Moreover, the shape of a keratin dimer can change depending on its environment (e.g. temperature, pH, etc.). Electron microscopy

has shown that the keratin IF has a diameter between 7 to 12 nm, and this range is the result of the characteristics described above. [5]

1.3 HUMAN HAIR GROWTH

Hair growth is a process that cycles between resting and growing. If a particular follicle's fiber is done growing, the hair falls out, and is then replaced by a new hair. This process is not very obvious in human hair, but is very obvious in animals that have a summer coat and a winter coat [6].

The hair follicle grows below the bottom layer of the epidermis (cells covering the human body) and out through a dermal papilla (connects the dermis to the epidermis and forms a ridge) [6]. Below the skin the hair follicle looks similar to a plant bulb growing in soil. Mitotic (cell division) activity helps the follicle to produce growth through the dermal papilla. Dermal papilla cells produce large amounts of keratin in their cytoplasm, become elongated, and essentially fill themselves with self-assembled bundles of IF held together with a matrix of keratin-associated proteins. This composite structure of proteins contains unusually large amounts of the amino acid cysteine, which has a pendant thiol group that can crosslink with another cysteine and form a disulfide bridge, a structure replete in nature for stabilizing proteins. Continued growth within the lower region of the follicle pushes the forming hair fiber outside the skin and exposes it to the oxygen in the air, which catalyzes the reaction of two thiols on proximal cysteines, a process known as "keratinization." This keratinization grows to the shape of a hollow cone which is about two-thirds the size of the follicle. Then, the keratinized cells that are growing in the hollow part break through the tip. As the hair grows, only the lower one-third to one-half of the

follicle remains mitotically active. Over time, the bulb of the hair follicle becomes two halves, upper and lower. The upper half, which includes the melanin (color) pigment, stops mitotic activity, while the lower half is still active; however, this half does not have any melanogenic pigments [6].

In the anagen (active follicle) stage there is an abundance of thiols and mitotic activity. In the telogen (resting follicle) stage there are not as many thiols as in anagen, only in the partially keratinized cells where there is mitotic activity. In the catagen stage the mitotic activity stops, so the hair is no longer growing. This process will start all over again to continue the cycle [6], [7].

1.4 STRUCTURE

Based on scattering studies, Feughelman proposed a model of what he believed is the structure of keratin IF, as well as the hierarchical nature of a wool fiber, which is similar to human hair fibers. He presents a structure in which many thin, parallel cylinders are fused together by a matrix to form the keratin fiber cortex, which is surrounded by a cuticle composed of flattened, overlapping cells [8]. Figure 1.1 below depicts the cuticle, cortex, and matrix described above.

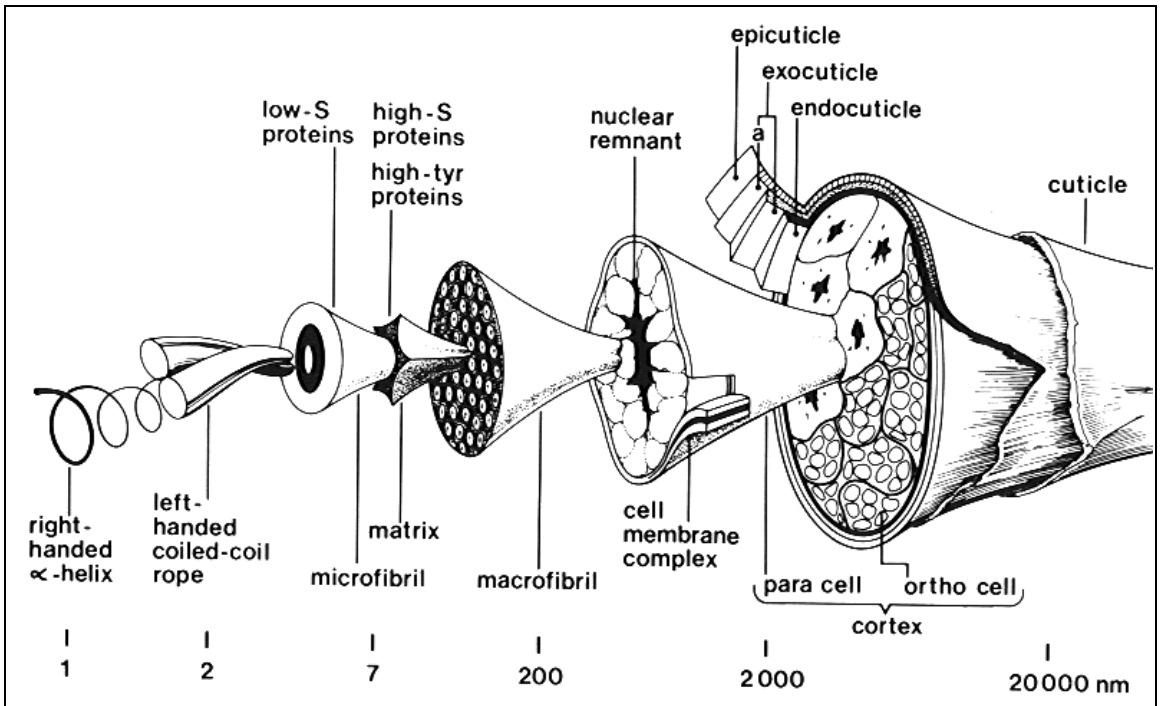

Figure 1.1 Schematic of a wool fiber. Human hair has a similar superstructure but varies in the ratio of matrix to microfibril proteins. [Copyright CSIRO Australia 1996. Reproduced with permission from The Lennox Legacy (Rivett DE, Ward SW, Belkin LM, Ramshaw JAM and Wilshire JFK. Published by CSIRO PUBLISHING, Melbourne Australia)]

Pauling et al. suggested that the fiber mentioned above could not be straight because we know that keratin is made up of repeating different kinds of amino acids. This helical shape builds the shape of the fiber about 400 Angstroms in length (40 nm) with an alpha helical arc of 5.2 Angstroms (0.52 nm). Figure 1.2 below illustrates the fiber is one strand in the middle with an alpha helical shape that has six strands twisted around it to be a total of 30 Angstroms in diameter (3 nm) [9].

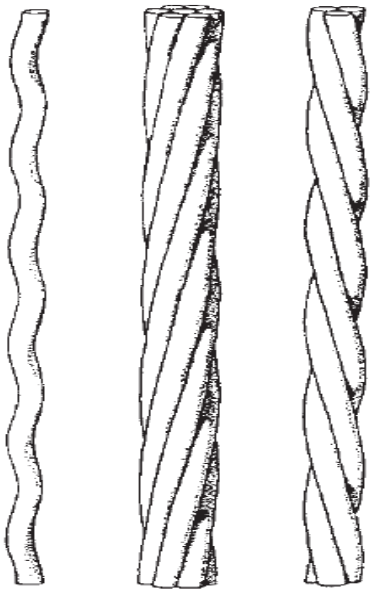

Figure 1.2 Alpha helical pitch of keratin. The keratin is wrapped around other keratin strands shown in the middle and right pictures. Reprinted by permission from Macmillan Publishers Ltd: [Nature] (L. Pauling and R. B. Corey, "Compound helical configurations of polypeptide chains: structure of proteins of the α-keratin type," *Nature,* vol. 171, 1953.), copyright (1953)

Aebi has a model that shows the keratin monomer looks similar to a rod with a large sphere on one end (tail end) and a small sphere on the other end (head end) represented in Figure 1.3 below. The tail region is carboxyl-terminal (-COOH) [4] and the head region amino-terminal (-NH2) [4]. Between the tail region and the middle of the strand is a coil and between the middle and the head region is another coil. The head region of one monomer attracts to the head region of another monomer, and likewise the tail regions are attracted to each other. This attraction causes the two monomers to join and form a dimer.

The two tails of one dimer are attracted to the two heads of another dimer, and once joined, they form a tetramer. Aebi also suggests that the tetramers can be oriented the other way and/or have the two dimers staggered. He calls this "tetramer switching." The two tetramers form dimers that can range from 50 nm long to 75 nm long [10].

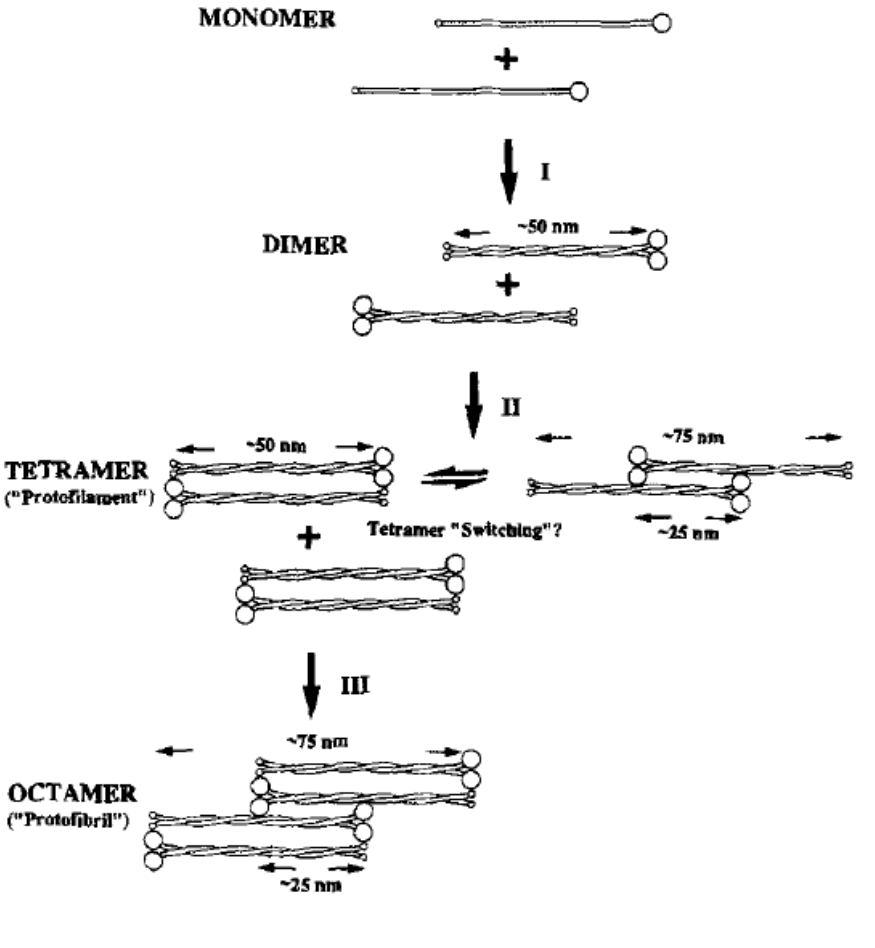

Figure 1.3 Assembly of two monomers to form a dimer. Used with permission [10] U. Aebi, M. Häner, J. Troncoso, R. Eichner, and A. Engel, "Unifying principles in intermediate filament (IF) structure and assembly," *Protoplasma*, vol. 145, pp. 73-81, 1988. Used with kind permission from Springer Science and Business Media, 2015.

Aebi also describes the monomer, depicted in Figure 1.4 below, as having three spaces in the middle that are non-α-helical. These spaces link the three α-helical regions together. The spacers are called L1, L12, and L2, and the helical regions are called 1A,

1B, 2A, and 2B [10]. The composite structure of hair fibers is important to consider because different regions of the cortex (i.e. microfibrillar versus matrix) will demonstrate different reaction kinetics due to the differences in molecular order.

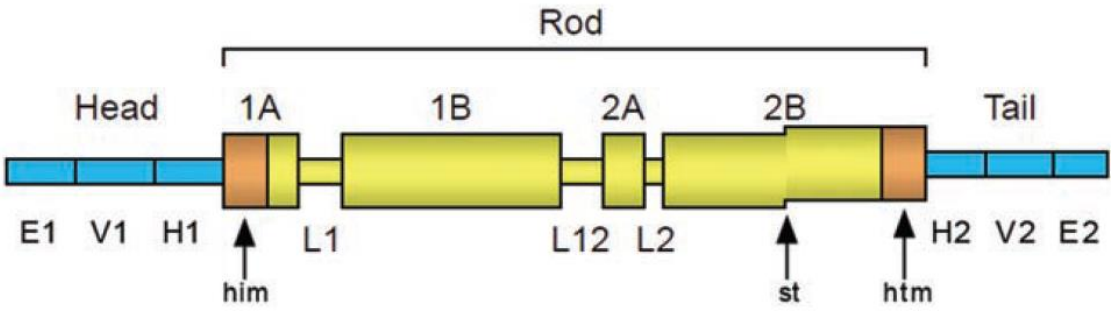

Figure 1.4 A keratin monomer. The monomer has a head, tail, and rod region. H1 and H2 are the homologous subdomain, V1 and V2 are the variable subdomain, and E1 and E2 are the end subdomain. Used with permission [11] H. H. Bragulla and D. G. Homberger, "Structure and functions of keratin proteins in simple, stratified, keratinized and cornified epithelia," *Journal of anatomy*, vol. 214, pp. 516-559, 2009. Used with kind permission from John Wiley and Sons, 2015

1.5 SELF-ASSEMBLY OF CORTEX

Intermediate Filaments (IF) form the bulk of the fiber cortex and are made up of protofilaments (linear polymer of tetramers) or protofibrils (linear polymer of octamers). In different environments, protofilaments may aggregate together looking like half staggered octamers [10]. This form of aggregation is driven by the primary and secondary structure of the proteins, like pieces of a puzzle fitting together, and the energy of the system. In nature these environments can be highly controlled at the sub-cellular level but are challenging to control within extracted keratin solutions. Therefore, re-forming keratins into biomaterials via such self-assembled processes is challenging and has not been extensively studied.

Crewther stated “hard alpha-keratin and epidermal keratin show that interchain ionic interactions are maximized when two chains aggregate in parallel rather than in an anti-parallel manner [5].” Crewther also proposes four different anti-parallel assembly structures for keratin tetramers, represented in Figure 1.5 below, and how they vary in size from about 44 nm to 70 nm [5].

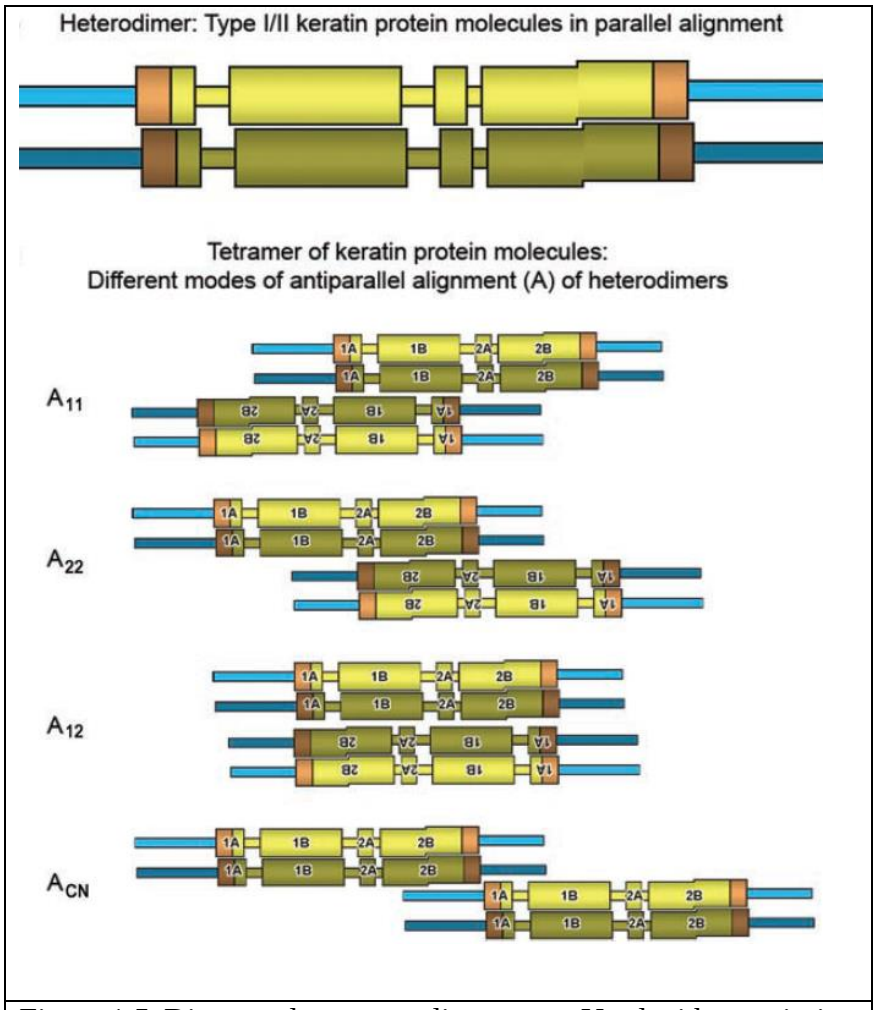

Figure 1.5 Dimer and tetramer alignments. Used with permission [11] H. H. Bragulla and D. G. Homberger, "Structure and functions of keratin proteins in simple, stratified, keratinized and cornified epithelia," *Journal of anatomy*, vol. 214, pp. 516-559, 2009. Used with kind permission from John Wiley and Sons, 2015

Hermann et al. performed an experiment that showed the influence that buffer conditions can have on molecular size. Epithelial keratins (K8 and K18) in 2 mM Tris-HCl (pH 9.0) and 20 mM Tris-HCl (pH 7.0) were much shorter than the keratins in 100 mM NaCl, 40 mM Tris-HCl (pH 7.0), and 5 mM Tris-HCl (pH 8.4). The shorter keratins ranged from 50 to 120 nm, with majority at 50, 75, 100, and 120 nm. The assembly process for the longer filaments happened in 10 seconds [12].

Herman et al. performed another experiment that showed more head domains will influence aggregation. Using the same epithelial keratins as before, keratins in 5 mM Tris-HCl (pH 8.4) had lengths of 50 nm. When more head peptides of K8 or K18 were added to the solution the aggregation increased; however, when K8 was introduced to the solution a 20-40 nm diameter was observed. Even when two head terminals are "fused" together and added to the solution, aggregation increases [12].

Steinert performed an experiment with mouse epidermal keratin to see how fast keratin reassembled after being taken out of a solution of Urea. The highest concentration of 1.80 mg/mL reassembled the fastest and a concentration of 0.65 mg/mL reassembled the slowest. It was also observed that the initial rate produced a sigmoidal curve for most concentrations. It is suggested that instead of monomers, the initial step is formed by six-chain oligomers. The study also observed the change in length of the keratin fibers over time. At ten minutes the lengths were about 65 nm, at twelve minutes the lengths were 90-130 nm, and at sixteen minutes the lengths were long polymers [13].

These studies demonstrate that while some work has been done to determine the structure of monomers and oligomers that form early in the process of fiber cortex creation, relatively little data exists that demonstrates how these grow to generate IF during hair

morphogenesis. Moreover, the properties of isolated oligomers is not extensively characterized either.

1.6 EXTRACTION

To understand both the behavior of extracted human hair keratins, as well as how purified solutions may assemble to form biomaterials such as hydrogels, a discussion of the extraction process itself is warranted. Keratins can be extracted by two different methods to produce what are typically referred to as "kerateine" or "keratose." As a protein family, keratins are distinguished by their high sulfur content and extensive disulfide crosslinking. It is this high level of disulfide crosslinking, particularly in the head and tail regions, that makes keratin structures tough and durable, and as a result, difficult to un-crosslink and solubilize. To break the disulfide bonds (as opposed to the backbone polypeptide bonds), either reducing or oxidizing agents are used. When reducing agents are used, the resulting keratins retain thiol functionality at the cysteine amino acid; when oxidizing agents are used, the disulfide bonds are converted to different forms of oxo-cysteine, which in most cases is the fully oxidized cysteic acid form (i.e. SO_3^-). Table 1 below compares the differences between the two general extraction methods.

Table 1 Comparison of general kerateine and keratose extractions

Kerateine [14]	Keratose [15]
1 M Thioglycolic acid at pH 10 for 12 hours to break disulfide bonds and extract proteins	2% peracetic acid for 10 hours to break disulfide bonds
100 mM Trise base to further extract proteins	100 mM Trise base for 2 hours to extract proteins
Ultrapure water to further extract proteins	Ultrapure water to further extract proteins
Clarify extract by centrifugation and filtration	Clarify extract by centrifugation and filtration
Dialysis for purification	Dialysis for purification

Shin et al. did an experiment to see if microwave assisted extractions could speed up the extraction time for kerateines. He made the same set of solution using the so-called "Shindai" method. The Shindai method uses 25 mM Tris-HCl (pH 8.5), 2.6 M Thiourea, 5 M Urea, and 5% 2-Mercaptoethanol (reducing agent). This is different from the conventional method that uses 8 M Urea instead of 5M and no thiourea [16]. In Shin et al.'s experiment, one solution sat for 24 hours while the other was in the microwave for 2 hours. After about 60 min in the microwave the keratin proteins start to degrade; however, it resulted in about the same yield as the solution sitting for 24 hours [17]. Nakamura et al. did an experiment to compare the two methods, Shindai and conventional. It was observed that all of the components from the Shindai method led to extractions with more yield from human hair, human nail, wool, rat hair, and chicken feather than the conventional method [16]. In general, these methods are similar but subtle differences can effect reaction kinetics. Also, because peptide hydrolysis is present as a side reaction in any of these processes, all reactions produce some amount of by-products.

Franbourg et al. performed a study comparing the ethnic differences of human hair that had not been chemically treated, or "virgin" hair. Chemically treated refers to dyeing, perming, and chemically straightening one's hair. Asian, Caucasian, and African are the three major ethnic origins and the ones studied. This study showed that during an X-Ray analysis all three ethnic origins have the same chemical composition and keratin structure. There are, however, three major differences in radial swelling and tensile strength. African hair swells the least amount and has the lowest tensile strength. Caucasian hair swells the most, and Asian hair has the highest tensile strength [18]. The present work uses virgin

Asian hair. The radial swelling and breakage is important during the extraction process and this will also effect reaction kinetics.

Figure 1.6 below taken with a scanning electron microscope (SEM) compare the difference between the hairs before extraction to the hair after extraction. Since hair swells when submerged in a liquid, we expect to see the hair's diameter be larger than the original. Because of the radial swelling we also expect to see the hair break/split down the side [15].

Magnification	Virgin Hair	Kerateine Extraction	Keratose Extraction
200x (Region 1)	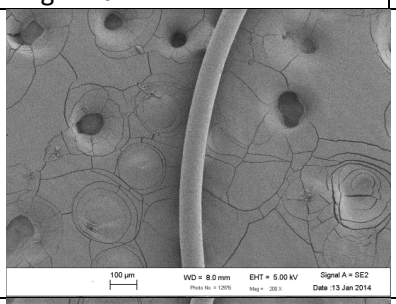	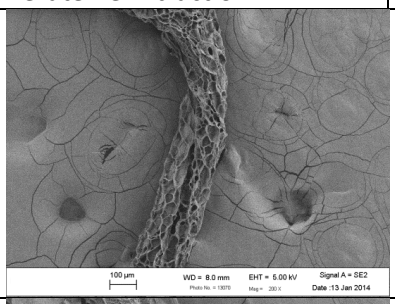	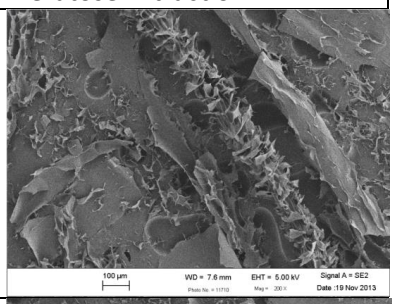
200x (Region 2)	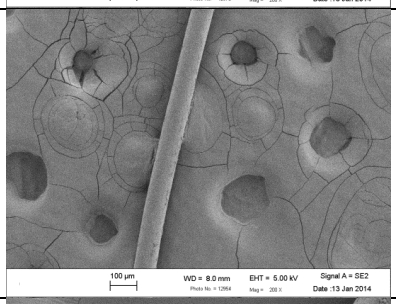	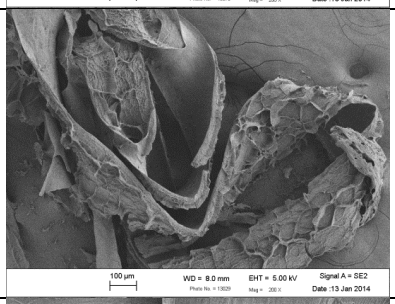	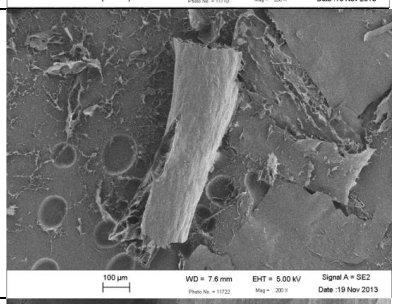
1000x (Region 3)	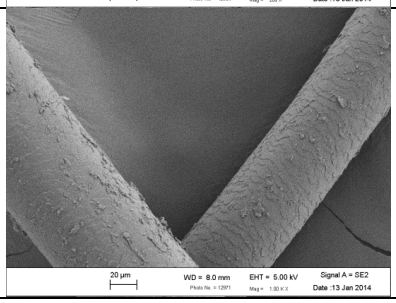	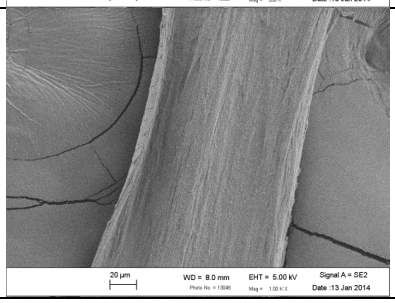	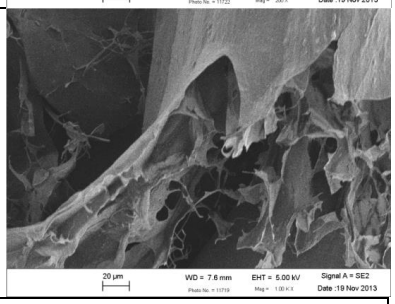

Figure 1.6 Human hair before and after extraction. The left column demonstrates a strand of human hair before either type of extraction process. The middle column demonstrates the hair after a kerateine extraction (reductive), while the right column demonstrates after keratose (oxidative).

During an oxidative extraction (i.e. one that produces keratose), the oxidant breaks the disulfide bonds that stabilize the cortical protein composite structure [19]. When a kerateine (ending coming from the word cysteine) extraction is performed, the disulfide

bond breaks and forms a thiol (-SH). However, when a keratose extraction is taking place the disulfide bond breaks and forms a sulfonic acid (-SO3H). Keratose tends to be more water soluble due to the polarity of the sulfonic acid groups. Kerateine can be re-crosslinked by oxidizing the thiol groups back to disulfide bonds such as when you expose kerateines to the oxygen in air. Kerateine is therefore covalently crosslinked (as opposed to keratose, which forms gel networks by entanglement), which tends to act like vulcanized rubber in that it is difficult to un-crosslink without degrading the material [20]. There are numerous other nuances to kerateines and keratoses, and different properties that relate to their underlying molecular structure. The majority of this thesis work is focused on kerateines as these are a useful building block for self-cross-linked structures. While it is important to develop a fundamental understanding of the self-assembly mechanisms of both kerateine and keratose, it is equally important to determine the fundamental solution behavior of extracted keratins in general, and kerateines, along with purified kerateine's core dimer structure in particular, to better understand how these materials may be isolated from complex extracts on the one hand, and processed into useful biomaterials on the other. To do so, the thesis work described in subsequent chapters utilized dynamic light scattering to investigate size and aggregation behavior of purified kerateine.

1.7 DYNAMIC LIGHT SCATTERING

Light scattering is a technique used to measure the size of particles which can lead to understanding molecular assemblies such as aggregation [21]. It can be split into two categories: static and dynamic. The main difference between the static and dynamic techniques is in the length of time necessary to detect the size. Static light scattering

measures the size in seconds, whereas dynamic light scattering measures the size in microseconds [21]. This thesis work focuses on dynamic light scattering (DLS), also referred to as photon correlation spectroscopy (PCS) or quasi-elastic light scattering (QLS) [21], [22], [23].

Dynamic light scattering is a noninvasive technique that measures particles in the sub-micron region while they are in solution undergoing Brownian motion [21], [22], [23]. Brownian motion is the consistent random movement of the solute particles because of the consistent collisions with the solvent particles.

1.7.1 Size calculation: While the particles are randomly moving in solution, a laser beam is aimed towards the particles. When the laser comes into contact with the particles in solution, the energy is absorbed and later released as a photon traveling in some arbitrary direction. Because the photons are emitted by particles undergoing Brownian motion, the Doppler Effect causes the photons to have different frequencies while traveling towards the detector [22], [21], [23].

The current study uses a Zetasizer Nano ZS. The setup is illustrated below in Figure 1.7. A laser, with a wavelength of 532 nm, is first projected through an attenuator. The attenuator is made up of an iris and a lens. After the attenuator, the laser goes through the sample. This instrument has an Avalanche photodiode detector at an angle of 173° relative to the original laser beam direction [22], [24]. The Avalanche photodiode detector is a new detector that finds signals with lower power lasers. This helps protect the sample from overheating from higher power lasers [22]. The instrument also features a Peltier element to heat and cool the sample for temperature control [24].

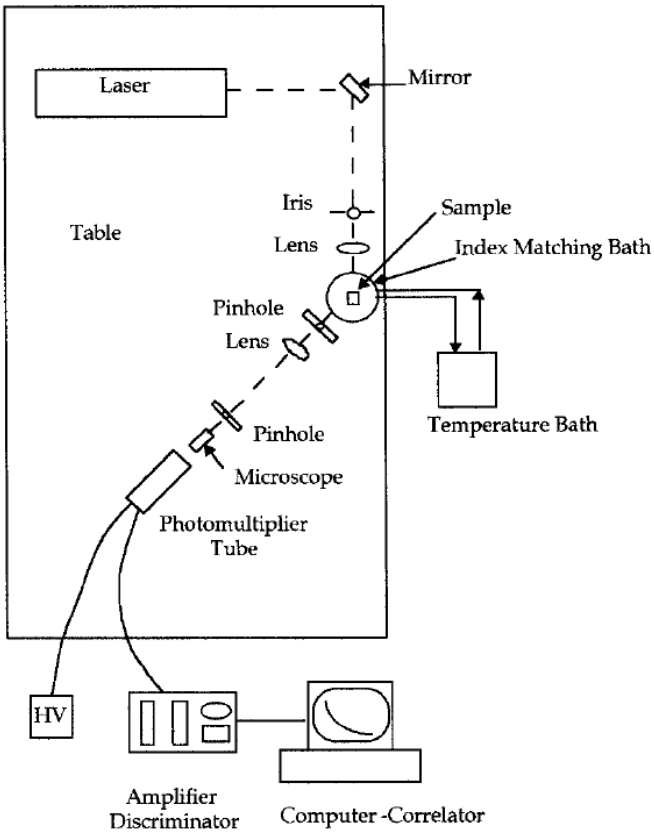

Figure 1.7 Dynamic light scattering instrument setup. Used with permission [22] R. Pecora, "Dynamic light scattering measurement of nanometer particles in liquids," *Journal of nanoparticle research*, vol. 2, pp. 123-131, 2000. Used with kind permission from Springer Science and Business Media, 2015.

After the detector collects all of the photon intensities over some time period (assuming a stationary data set so the data's trends do not change with time), the instrument auto-correlates the data and normalizes this based on (Eq 1.1) where $C(t)$ is the intensity autocorrelation function, γ is the coherence of the instrumental setup, $g^{(1)}(t)$ is the first order time autocorrelation function [22], [25].

$$C(t) = \frac{\langle I(t)I(0)\rangle}{\langle I(0)I(0)\rangle} = \left[1 + \gamma\left[g^{(1)}(t)\right]^2\right] \quad \text{Eq 1.1}$$

The first order time autocorrelation function is derived from a Fourier transform (which shifts data from the time domain to the frequency domain). Equation 1.2 is a single exponential for a solution of monodispersed nanoparticles where q is the scattering vector length and D is the diffusion coefficient [21], [22], [25].

$$g^1(t) = e^{-q^2 Dt} \quad \text{Eq 1.2}$$

To calculate the scattering vector length, Equation 1.3 is used where λ is the wavelength and θ is the scattering angle [21], [22], [25] .

$$q = \frac{4\pi}{\lambda} \sin\left(\frac{\theta}{2}\right) \quad \text{Eq 1.3}$$

From the known diffusion coefficient, the size of the particle can be determined using the Stokes-Einstein equation where k_B is Boltzmann's constant, T is temperature, η is solvent viscosity, and R is solute radius [21], [22], [25].

$$D = \frac{k_B T}{6\pi\eta R} \quad \text{Eq 1.4}$$

The Stokes-Einstein equation (Eq 1.4) above assumes the nanoparticle is a sphere; therefore, when the nanoparticle is non-spherical the radius is called the hydrodynamic radius, which is not the geometrical radius [22].

1.7.2 Polydispersity: Polydisperse samples have multiple sizes and shapes, which lead to different diffusion coefficients. Using the first order correlation function where D_i is a given diffusion coefficient and A_i is the weighting factor proportional to the scattered intensity, Equation 1.5 is now a sum of exponentials [22].

$$g^{(1)}(t) = \sum_i A_i e^{-q^2 D_i t} \quad \text{Eq 1.5}$$

Using the cumulants method, Equation 1.6 is expanded using a power series. A computer program calculates the first few cumulants, K_1 and K_2. K_1 is the average reciprocal relaxation time and K_2 is dispersion reciprocal relaxation time [22].

$$\ln\left[g^{(1)}t\right] = -K_1 t + \left(\frac{1}{2}\right) K_2 t^2 \qquad \text{Eq 1.6}$$

1.8 APPLICATION OF DLS TO KERATIN SOLUTIONS

Like other structural proteins, keratins can exist in several forms in solution from individual molecules to multi-molecule aggregates. Since keratins are a self-assembling protein family, they possess an intrinsic ability to associate with themselves in a specific manner. However, since extracted keratins can be damaged, random assemblies can also occur. The desire to understand the extent to which extracted (and then purified) keratin preparations behave in solution, particularly with regard to aggregation, and the solution conditions in which this occurs or can be minimized, is the primary motivation for this thesis research. DLS provides convenient means to test extracted/purified keratin solutions under varying conditions of buffer type, concentration, pH, time, and temperature. The goal of this research is to investigate these solution parameters and determine the extent of protein aggregation and size of aggregates by DLS.

CHAPTER 2 -EXPERIMENTAL

2.1 INTRODUCTION

Keratin biomaterials is observed to show signs of aggregation in the same environmental conditions as other proteins. Collagen (a protein found in hide and skin) aggregates heavily in Ultrapure water because of the ionic substituents [26]. Aggregation can lead to multiple complications when it comes to purification during extraction. As mentioned in the introduction (Table 1), whether it is kerateine or keratose, Ultrapure water is used in both types of extraction. Ultrapure water is used to eliminate any residue of the toxic chemicals used in the initial sets of extraction. Also, Ultrapure water is used to finish the purification during extraction. If the keratin proteins are aggregating then unwanted material may not filter out during dialysis. Unwanted material refers to head or tail regions without a rod domain. The unwanted materials will affect the different applications that will use keratin, such as hydrogels, thin films, etc. The unwanted aggregation in hydrogels can influence the gel to have a weak structure resulting in early failure.

There is very little understanding on how keratins behave in different environmental solutions under controlled condition and water. Therefore, DLS was the method chosen for this thesis because it will show the size of the proteins in solution. DLS can do multiple runs for as long as the operator wants which leads to an understanding of how the protein size changes over time. The DLS can also show how much of the particular size of the protein is in the solution. While the DLS is not a very sensitive technique it is able to determine the difference of two very distinct sizes. These two sizes are useful in this thesis, so the smaller size is referred to as peak 1 and the larger size is referred to as peak 2.

The overall hypothesis of this thesis is to test how buffer solutions will affect aggregation compared to Ultrapure water. The effects of buffer concentration, addition of salt, pH, and temperature on aggregation will also be observed. The main goal is to better understand how keratin reacts in different environmental conditions and if the solvents of extraction method are the most optimal for further applications.

2.2 METHODS

2.2.1 Keratin nanomaterial preparation: Reduced keratin ("kerateine") was extracted and purified from washed human hair fibers obtained from a commercial vendor. Briefly, 100 g of Chinese hair fibers were cut into approximately 1 inch lengths by hand with scissors and reduced with 2 L of 0.042M sodium sulfide plus 1M urea at 37^{o}C with gentle shaking for 1.5 hr. The hair was separated by 500 μm sieve and the liquid retained. The reduced hair fibers were further extracted with 2 L of 100 mM tris base by gentle shaking at 37^{o}C for 2 hr. The hair was again separated by sieve and the two extract solutions combined. Suspended solids were separated by centrifugation at 20K rpm and the solution filtered through No. 4 Whatman filter paper. The clarified solution was purified for 10 volume washes (ca. 80 L) of 10/100 mM disodium phosphate/sodium chloride at pH 9.3, followed by 5 volume washes of Ultrapure water in a custom-designed tangential flow filtration system utilizing a 100K Da nominal low molecular weight cutoff membrane, which removed contaminating peptides and processing reagents, and yielded a purified sample of keratin nanomaterial. A sample of the purified solution was removed for analysis of total protein content by the Lowry method (see Section 2.2.3 below), which was used to determine dilutions for DLS analysis.

2.2.2 Test solution preparation: After purification, the sample was diluted to two concentrations, 0.1 mg/mL (0.01%) and 0.5 mg/mL (0.05%) into Ultrapure water and three different buffer solutions: 10 mM HNa_2PO_4, 100 mM HNa_2PO_4, and 10/100 mM HNa_2PO_4/NaCl. All buffer solutions were further aliquoted and titrated to pH's of 7.4, 8.0, 8.5, and 9.0. Three milliliters of each sample were used to analyze by dynamic light scattering (DLS) at three different temperatures. Aebi et al. found that 1-15mM HNa_2PO_4 unravels proteins at neutral pHs [27]. This study expanded on the results by studying 10 mM and 100 mM while also expanding the pH range.

2.2.3 Lowry total protein assay: Lowry assay is a method to determine protein concentration in an aqueous solution. In order to generate a standard curve, a 10 mg/mL solution of albumin bovine serum (BSA) in Ultrapure water was serially diluted, then 5 μL was pipetted into a 96 well plate along with 5 μL of keratin. Reagent A (25 μL) and Reagent B (200 μL) were added to change the color of the protein solution based on concentration. Reagent A is 2% Na_2CO_3 in 0.1 M NaOH and Reagent B is 0.5% $CuSO_4$+$5H_2O$ in 1% Na or K tartate [28]. The 96 well plate is then incubated in a dark space for 15 minutes at room temperature. The 96 well plate was put inside a plate reader and read at wavelength 750 nm. Table 2 below shows the absorbance readings for BSA. The numbers in red were excluded in the averaged data due to pipetting error.

Table 2 Absorbance readings of albumin bovine serum					
Concentration (mg/mL)	Albumin Bovine Serum	Albumin Bovine Serum	Albumin Bovine Serum	Albumin Bovine Serum	Average
10	0.895	0.88	0.873	0.872	0.88
5	0.592	0.609	0.605	0.626	0.608
2.5	0.406	0.426	0.338	0.406	0.412667
1.25	0.238	0.257	0.262	0.255	0.253
0.625	0.182	0.241	0.176	0.162	0.173333
0.3125	0.116	0.128	0.126	0.122	0.123
0.15625	0.099	0.097	0.1	0.101	0.09925
0.078125	0.083	0.088	0.09	0.085	0.0865

Figure 2.1 below shows the absorbance readings vs. concentration to find a linear fit regression line. The equation is used to calculate the concentration of keratin. This is possible because we know the absorbance reading of keratin.

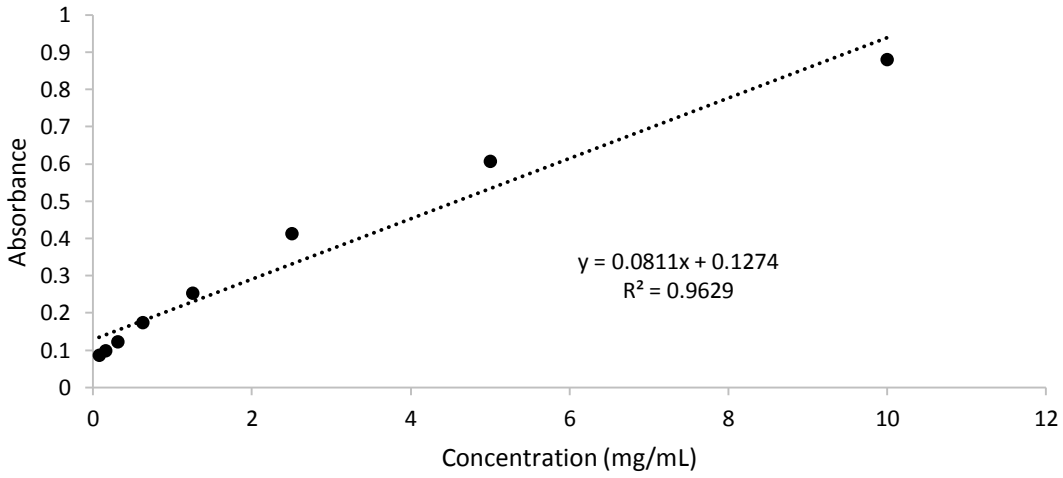

Figure 2.1 Absorbance vs. Concentration of Albumin Bovine Serum

Table 3 below shows the absorbance readings for kerateine. The sample readings below are of an unknown kerateine concentration. The standard curve equation will be

used to determine the concentration. The numbers in red are excluded due to pipetting error.

Table 3 Absorbance readings of kerateine at wavelength of 750 nm									
Keratin									Average
0.191	0.201	0.172	0.118	0.213	0.214	0.207	0.226	0.213	0.209

Using the linear equation from Figure 2.1 [i.e. concentration = (absorbance - 0.1274)/0.0811], determinations of concentration in the unknown keratin solution were made as shown in Table 4.

Table 4 Calculated keratin concentration values for replicate samples									
=(y-0.1274)/0.0811									Average
0.784	0.908	0.550	-0.116	1.055	1.068	0.982	1.216	1.055	1.010

2.2.4 Dynamic light scattering (DLS): The DLS measurements were obtained using a Zetasizer ZS. One milliliter of keratin in each buffer was placed into a disposable plastic cuvette and then placed into the instrument. Each sample equilibrated for ten minutes before measurements began. The equilibration time ensured the sample matched the temperature being tested: 4°C, 25°C, and 37°C. Seven measurements were taken for each sample to ensure stability over 20 to 30 minutes at that temperature.

2.2.5 Statistical methods: Ten samples were chosen at random to test for normality. Normality means the samples have a Gaussian distribution. The statistical software package, JMP from the SAS Institute, was used for evaluation of all data. Table 5 shows the results from this software. The conclusion cannot be drawn that all samples have a

normal shape. Therefore, the Levene test for equal variances was used to see if there is a statistically significant difference in experimental outcomes between sample solution conditions because it is the least sensitive test and it does not assume normality. The DLS was programmed to acquire data for seven replicates of the same sample over a 20-30 minute period. These data were tested by the instrument software against internal quality control measures and reported as number intensity vs. size, as well as volume intensity vs. size; volume intensity data was used to determine relative amounts of different sized aggregates. The DLS software calculated the following values from these curves: number intensity peak 1 mean size, number intensity peak 2 mean size, etc., volume intensity peak 1 area, volume intensity peak 2 area, etc. for each of the 7 replicate analyses of single solution samples. Mean and standard deviations for each of the samples was calculated from these 7 replicates using Excel. Standard deviation of the volume intensity data was considered a surrogate for aggregation as this value indicates the presence of numerous aggregates that contribute to sample complexity, which in turn prevents the sample from establishing optimal data acquisition settings and thus, consistent scattering intensity across all 7 replicates (i.e. large standard deviation indicates high aggregation; low standard deviation indicates low aggregation in the volume percent data).

Table 5 Tests for normality. X-axis shows size for the first two columns and percent for the second two columns. Y-axis shows how many are in that range.

0.5 mg/mL of Keratin in 10 mM HNa_2PO_4 pH 7.4 at Temperature 4			
Peak 1 Mean Intensity Size (d.nm)	Peak 2 Mean Intensity Size (d.nm)	Peak 1 Volume Percent	Peak 2 Volume Percent
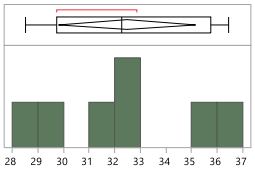	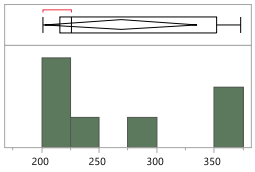	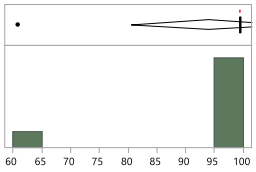	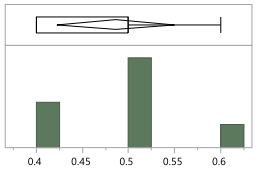
Normal	Bimodal	Left Skew	Normal
0.1 mg/mL of Keratin in 10 mM HNa_2PO_4 pH 9 at Temperature 4			
Peak 1 Mean Intensity Size (d.nm)	Peak 2 Mean Intensity Size (d.nm)	Peak 1 Volume Percent	Peak 2 Volume Percent
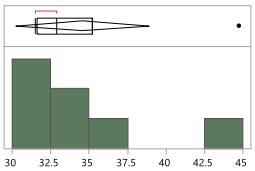	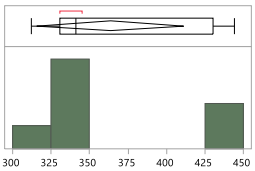	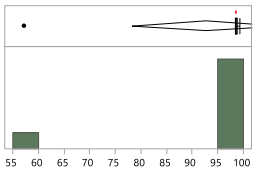	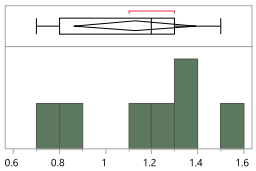
Right Skew	Right Shew	Left Skew	Left Skew
0.1 mg/mL of Keratin in 10/100 mM HNa_2PO_4/NaCl pH 8.5 at Temperature 4			
Peak 1 Mean Intensity Size (d.nm)	Peak 2 Mean Intensity Size (d.nm)	Peak 1 Volume Percent	Peak 2 Volume Percent
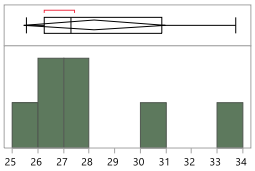	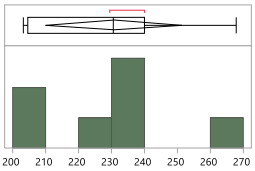	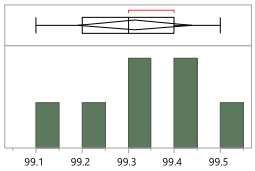	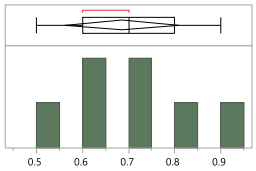
Right Skew	Normal	Normal	Normal
0.5 mg/mL of Keratin in 100 mM HNa_2PO_4 pH 8 at Temperature 4			
Peak 1 Mean Intensity Size (d.nm)	Peak 2 Mean Intensity Size (d.nm)	Peak 1 Volume Percent	Peak 2 Volume Percent
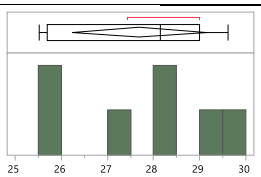	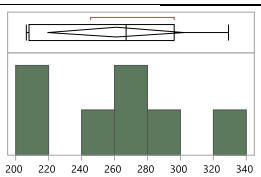	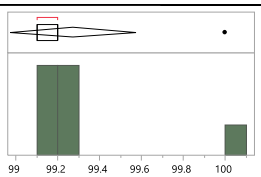	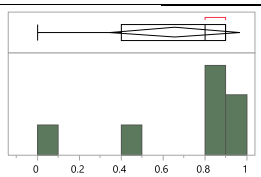
Bimodal	Bimodal	Right Skew	Left Shew

0.5 mg/mL of Keratin in Ultrapure Water at Temperature 4			
Peak 1 Mean Intensity Size (d.nm)	Peak 2 Mean Intensity Size (d.nm)	Peak 1 Volume Percent	Peak 2 Volume Percent
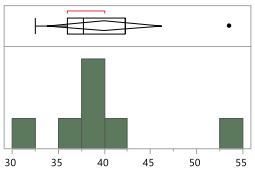	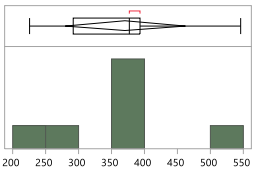	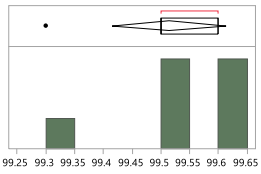	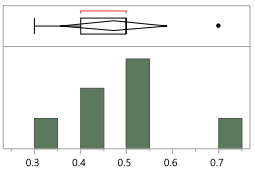
Normal	Normal	Left Skew	Normal
0.1 mg/mL of Keratin in 10 mM HNa_2PO_4 pH 9 at Temperature 25			
Peak 1 Mean Intensity Size (d.nm)	Peak 2 Mean Intensity Size (d.nm)	Peak 1 Volume Percent	Peak 2 Volume Percent
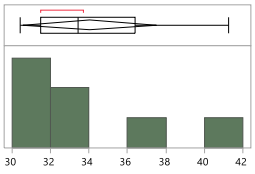	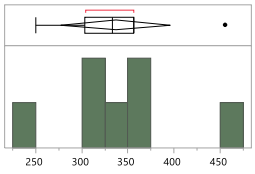	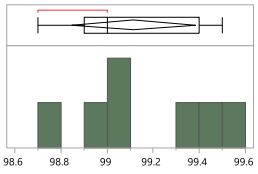	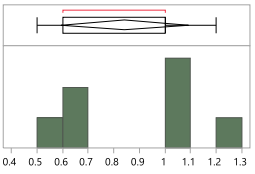
Right Skew	Bimodal	Normal	Left Skew
0.5 mg/mL of Keratin in 10/100 mM HNa_2PO_4/NaCl pH 8 at Temperature 25			
Peak 1 Mean Intensity Size (d.nm)	Peak 2 Mean Intensity Size (d.nm)	Peak 1 Volume Percent	Peak 2 Volume Percent
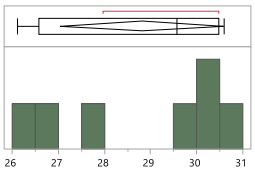	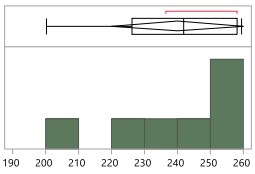	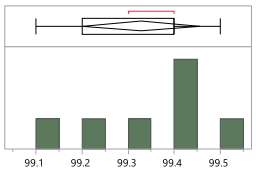	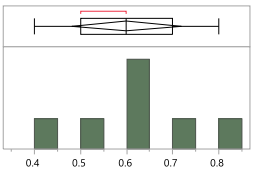
Left Skew	Left Skew	Left Skew	Normal
0.5 mg/mL of Keratin in 100 mM HNa_2PO_4 pH 7.4 at Temperature 25			
Peak 1 Mean Intensity Size (d.nm)	Peak 2 Mean Intensity Size (d.nm)	Peak 1 Volume Percent	Peak 2 Volume Percent
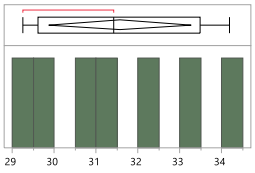	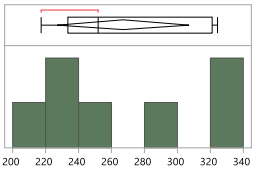	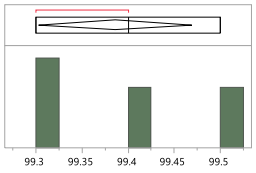	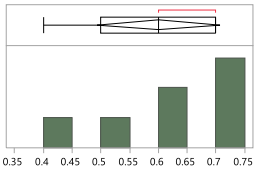
Plateau	Bimodal	Right Skew	Left Skew

0.5 mg/mL of Keratin in 10/100 mM HNa_2PO_4/NaCl pH 7.4 at Temperature 37			
Peak 1 Mean Intensity Size (d.nm)	Peak 2 Mean Intensity Size (d.nm)	Peak 1 Volume Percent	Peak 2 Volume Percent
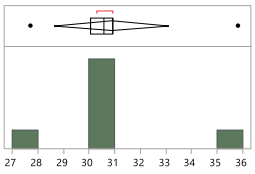	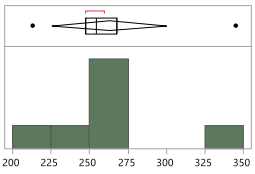	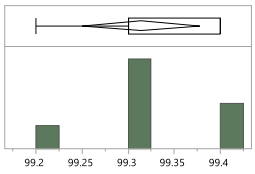	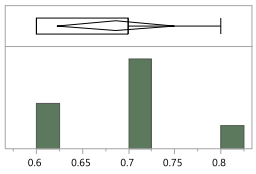
Normal	Normal	Normal	Noraml
0.5 mg/mL of Keratin in 10/100 mM HNa_2PO_4/NaCl pH 9 at Temperature 37			
Peak 1 Mean Intensity Size (d.nm)	Peak 2 Mean Intensity Size (d.nm)	Peak 1 Volume Percent	Peak 2 Volume Percent
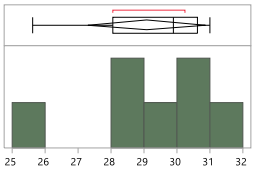	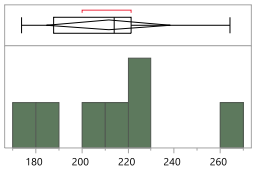	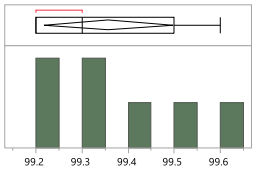	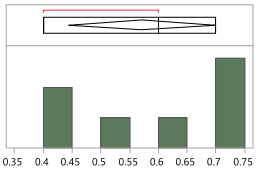
Bimodal	Normal	Right Skew	Bimodal

2.2.6 Analysis: Standard deviations of peak 1 volume percent were calculated for the seven runs within each sample. Volume percent was used because it is more representative of the number of particles at a particle size. Then the standard deviations were sorted from lowest to highest, then placed into JMP from the SAS Institute to see which ones fell in the 25%, 50%, 75%, and 90% quantile. If it is in the 25% quantile it means that the standard deviation is low and suggests little to no aggregation, while if it is in 90% quantile the standard deviation is high and suggests severe aggregation.

An example of volume percent graphs from the DLS output are shown in Figure 2.2, 2.3, 2.4, 2.5, and 2.6.

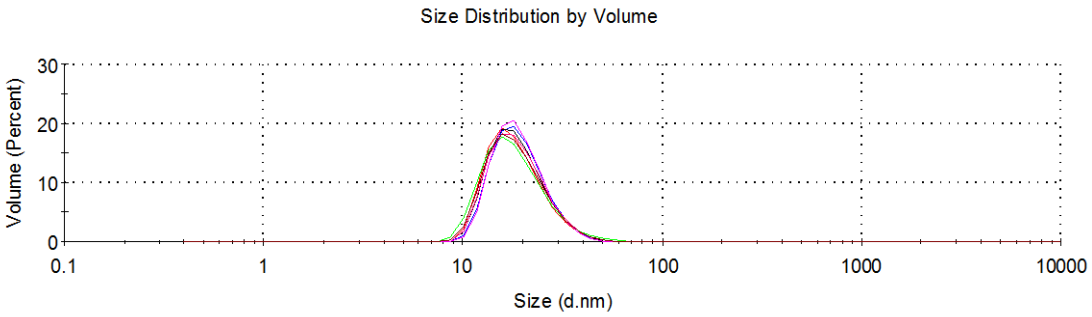

Figure 2.2 DLS spectrum for no aggregation. The picture represents the 0-25% quantile range of 0.1 mg/mL 10/100 mM HNa_2PO_4/NaCl pH 8.0 Temperature 4. The lack of multiple peaks and reproducibility of the seven replicate analyses of a single sample suggest little to no aggregation is occurring.

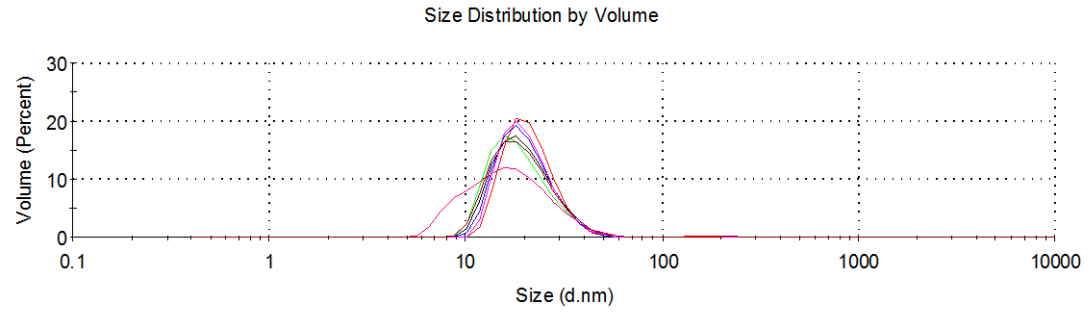

Figure 2.3 DLS spectrum for mild aggregation. The picture represents the 25-50% quantile range of 0.1 mg/mL 10 mM HNa_2PO_4 pH 8.5 Temperature 37. The lack of multiple peaks and mild non-reproducibility of the seven replicate analyses of a single sample suggests mild aggregation is occurring.

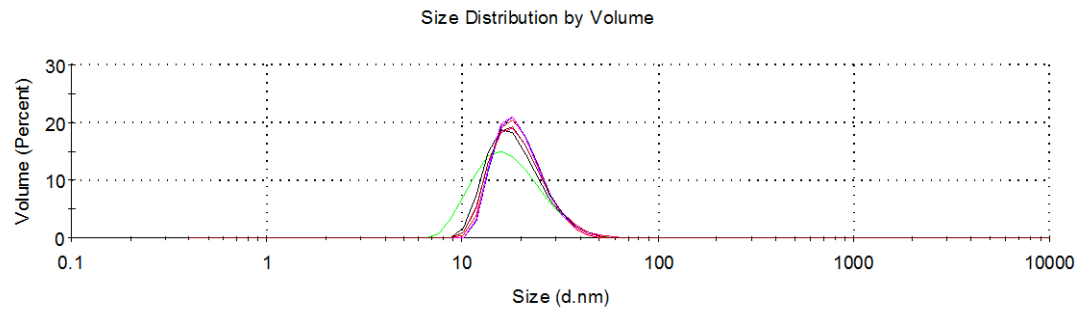

Figure 2.4 DLS spectrum for moderate aggregation. The picture represents the 50-75% quantile range of 0.1 mg/mL 10 mM HNa_2PO_4 pH 7.4 Temperature 37. The lack of multiple peaks and mild non-reproducibility of the seven replicate analyses of a single sample suggests moderate aggregation is occurring.

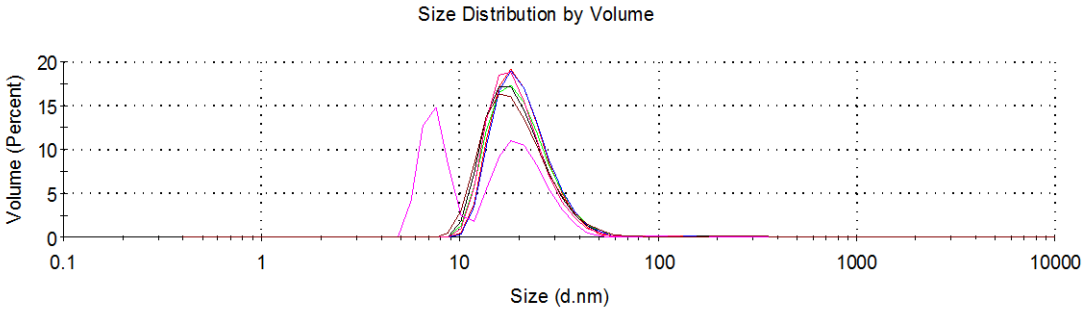

Figure 2.5 DLS spectrum for extensive aggregation. The picture represents the 75-90% quantile range of 0.1 mg/mL 10/100 mM HNa_2PO_4/NaCl pH 8.5 Temperature 25. The single presence of multiple peaks and moderate non-reproducibility of the seven replicate analyses of a single sample suggests extensive aggregation is occurring.

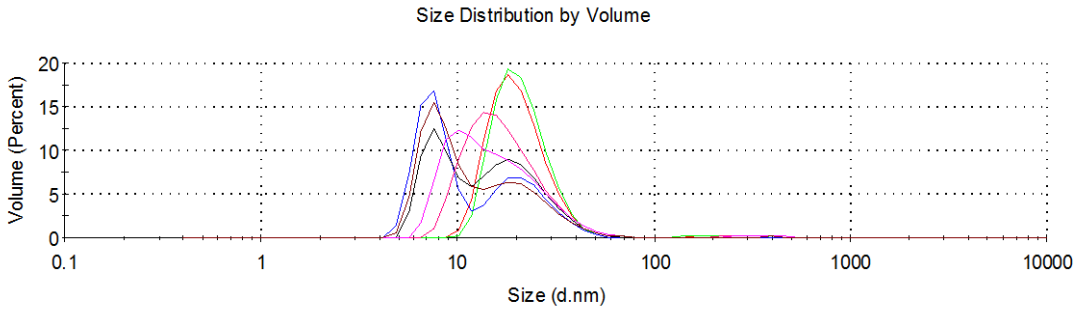

Figure 2.6 DLS spectrum for severe aggregation. The picture represents the 90-100% quantile range of 0.1 mg/mL Ultrapure Water Temperature 37. The presence of multiple peaks and lack of reproducibility of the seven replicate analyses of a single sample suggests severe aggregation is occurring.

2.3 RESULTS

To determine how keratin aggregates in buffer environments, a dynamic light scattering instrument was used to measure the sizes of the protein chains on the nanoscale. By looking at the standard deviation in the mass/volume percent graphs, it is possible to see if sample aggregation is occurring. If the standard deviation is high it means the DLS instrument had difficulty setting data acquisition conditions under which it could meet its quality criteria, which suggests a high level of sample composition complexity which in turn, may suggest a high level of protein aggregation.

The standard deviations for peak 1 volume percent were placed in order from least to greatest as shown in Table 6.

Table 6 List of samples with standard deviations

Sample Name	Standard Deviation	Percent Quantile	Aggregation
0.1 mg/mL of keratin in 10/100 mM HNa_2PO_4/NaCl pH 8.5 Temperature 37	0.048795		None
0.1 mg/mL of keratin in 100 mM HNa_2PO_4 pH 7.4 Temperature 4	0.069007		None
0.1 mg/mL of keratin in 10/100 mM HNa_2PO_4/NaCl pH 8.0 Temperature 37	0.069007		None
0.5 mg/mL of keratin in 10/100 mM HNa_2PO_4/NaCl pH 7.4 Temperature 37	0.069007		None
0.5 mg/mL of keratin in 10/100 mM HNa_2PO_4/NaCl pH 8.5 Temperature 37	0.069007		None
0.5 mg/mL of keratin in 10/100 mM HNa_2PO_4/NaCl pH 7.4 Temperature 25	0.075593		None

0.5 mg/mL of keratin in 10/100 mM HNa_2PO_4/NaCl pH 7.4 Temperature 4	0.07868		None
0.5 mg/mL of keratin in 10/100 mM HNa_2PO_4/NaCl pH 8.5 Temperature 25	0.07868		None
0.1 mg/mL of keratin in 10/100 mM HNa_2PO_4/NaCl pH 8.0 Temperature 4	0.07868		None
0.1 mg/mL of keratin in 10/100 mM HNa_2PO_4/NaCl pH 7.4 Temperature 37	0.08165		None
0.5 mg/mL of keratin in 100 mM HNa_2PO_4 pH 7.4 Temperature 25	0.089974		None
0.5 mg/mL of keratin in 10 mM HNa_2PO_4 pH 7.4 Temperature 25	0.09759		None
0.5 mg/mL of keratin in 10 mM HNa_2PO_4 pH 9.0 Temperature 37	0.09759		None
0.5 mg/mL of keratin in 100 mM HNa_2PO_4 pH 8.0 Temperature 37	0.098319		None
0.5 mg/mL of keratin in 10 mM HNa_2PO_4 pH 8.5 Temperature 4	0.106904		None
0.5 mg/mL of keratin in Ultrapure Water Temperature 4	0.106904		None
0.5 mg/mL of keratin in 10 mM HNa_2PO_4 pH 8.0 Temperature 37	0.106904		None
0.5 mg/mL of keratin in 100 mM HNa_2PO_4 pH 9.0 Temperature 37	0.106904		None
0.5 mg/mL of keratin in 100 mM HNa_2PO_4 pH 8.5 Temperature 37	0.11127	25%	None
0.1 mg/mL of keratin in 10/100 mM HNa_2PO_4/NaCl pH 9.0 Temperature 25	0.121499		Mild
0.5 mg/mL of keratin in 10/100 mM HNa_2PO_4/NaCl pH 9.0 Temperature 25	0.121499		Mild
0.5 mg/mL of keratin in 100 mM HNa_2PO_4 pH 9.0 Temperature 25	0.127242		Mild
0.1 mg/mL of keratin in 10 mM HNa_2PO_4 pH 7.4 Temperature 25	0.129099		Mild
0.1 mg/mL of keratin in 10/100 mM HNa_2PO_4/NaCl pH 8.0 Temperature 25	0.129099		Mild
0.1 mg/mL of keratin in 10/100 mM HNa_2PO_4/NaCl pH 8.5 Temperature 4	0.134519		Mild
0.5 mg/mL of keratin in 10/100 mM HNa_2PO_4/NaCl pH 8.5 Temperature 4	0.138013		Mild
0.5 mg/mL of keratin in 10/100 mM HNa_2PO_4/NaCl pH 8.0 Temperature 25	0.138013		Mild
0.1 mg/mL of keratin in 10 mM HNa_2PO_4 pH 8.5 Temperature 4	0.139728		Mild
0.1 mg/mL of keratin in 10 mM HNa_2PO_4 pH 8.5 Temperature 37	0.141421		Mild
0.5 mg/mL of keratin in 10 mM HNa_2PO_4 pH 8.5 Temperature 37	0.141421		Mild
0.5 mg/mL of keratin in 100 mM HNa_2PO_4 pH 8.5 Temperature 4	0.149603		Mild
0.5 mg/mL of keratin in 10/100 mM HNa_2PO_4/NaCl pH 9.0 Temperature 37	0.151186		Mild
0.5 mg/mL of keratin in 10 mM HNa_2PO_4 pH 8.0 Temperature 4	0.157359		Mild
0.1 mg/mL of keratin in 10 mM HNa_2PO_4 pH 7.4 Temperature 4	0.163299		Mild
0.5 mg/mL of keratin in 10 mM HNa_2PO_4 pH 9.0 Temperature 25	0.170434		Mild
0.5 mg/mL of keratin in 100 mMHNa_2PO_4 pH 8.5 Temperature 25	0.171825		Mild
0.1 mg/mL of keratin in 100 mM HNa_2PO_4 pH 8.5 Temperature 4	0.173205		Mild
0.1 mg/mL of keratin in 10 mM HNa_2PO_4 pH 8.0 Temperature 4	0.198806		Mild
0.1 mg/mL of keratin in 10 mM HNa_2PO_4 pH 8.0 Temperature 25	0.20702	50%	Mild
0.1 mg/mL of keratin in 10 mM HNa_2PO_4 pH 8.0 Temperature 37	0.21157		Moderate
0.1 mg/mL of keratin in 10 mM HNa_2PO_4 pH 9.0 Temperature 37	0.213809		Moderate
0.1 mg/mL of keratin in 100 mM HNa_2PO_4 pH 8.0 Temperature 4	0.222539		Moderate
0.1 mg/mL of keratin in 100 mM HNa_2PO_4 pH 7.4 Temperature 37	0.226779		Moderate
0.1 mg/mL of keratin in 100 mM HNa_2PO_4 pH 7.4 Temperature 25	0.237045		Moderate
0.5 mg/mL of keratin in 10 mM HNa_2PO_4 pH 8.0 Temperature 25	0.249762		Moderate

0.5 mg/mL of keratin in 10 mM HNa_2PO_4 pH 9.0 Temperature 4	0.257275		Moderate
0.5 mg/mL of keratin in 10/100 mM HNa_2PO_4/NaCl pH 9.0 Temperature 4	0.270801		Moderate
0.1 mg/mL of keratin in 10/100 mM HNa_2PO_4/NaCl pH 9.0 Temperature 37	0.276887		Moderate
0.5 mg/mL of keratin in 100 mM HNa_2PO_4 pH 8.0 Temperature 25	0.282		Moderate
0.1 mg/mL of keratin in 10 mM HNa_2PO_4 pH 7.4 Temperature 37	0.288675		Moderate
0.1 mg/mL of keratin in 10 mMHNa_2PO_4 pH 9.0 Temperature 25	0.291139		Moderate
0.5 mg/mL of keratin in 10 mM HNa_2PO_4 pH 8.5 Temperature 25	0.309377		Moderate
0.5 mg/mL of keratin in 10 mM HNa_2PO_4 pH 7.4 Temperature 37	0.318479		Moderate
0.1 mg/mL of keratin in 10/100 mM HNa_2PO_4/NaCl pH 7.4 Temperature 4	0.31997		Moderate
0.5 mg/mL of keratin in 100 mM HNa_2PO_4 pH 8.0 Temperature 4	0.325137		Moderate
0.1 mg/mL of keratin in 100 mM HNa_2PO_4 pH 8.5 Temperature 25	0.350238		Moderate
0.1 mg/mL of keratin in 100 mM HNa_2PO_4 pH 9.0 Temperature 37	0.394606		Moderate
0.5 mg/mL of keratin in 10/100 mM HNa_2PO_4/NaCl pH 8.0 Temperature 37	2.390557		Moderate
0.1 mg/mL of keratin in 10/100 mM HNa_2PO_4/NaCl pH 8.5 Temperature 25	4.74442	75%	Moderate
0.1 mg/mL of keratin in 10/100 mM HNa_2PO_4/NaCl pH 9.0 Temperature 4	5.107091		Extensive
0.5 mg/mL of keratin in 10/100 mM HNa_2PO_4/NaCl pH 8.0Temperature 4	8.203251		Extensive
0.1 mg/mL of keratin in 100 mM HNa_2PO_4 pH 8.0 Temperature 25	12.12111		Extensive
0.1 mg/mL of keratin in 10/100 mM HNa_2PO_4/NaCl pH 7.4 Temperature 25	12.39113		Extensive
0.5 mg/mL of keratin in 10 mM HNa_2PO_4 pH 7.4 Temperature 4	14.59589		Extensive
0.1 mg/mL of keratin in 10 mM HNa_2PO_4 pH 9.0 Temperature 4	15.76313		Extensive
0.1 mg/mL of keratin in 100 mM HNa_2PO_4 pH 8.5 Temperature 37	16.35374		Extensive
0.5 mg/mL of keratin in 100 mM HNa_2PO_4 pH 7.4 Temperature 4	16.4732		Extensive
0.1 mg/mL of keratin in Ultrapure Water Temperature 4	19.19268		Extensive
0.1 mg/mL of keratin in 100 mM HNa_2PO_4 pH 9.0 Temperature 4	21.13597		Extensive
0.5 mg/mL of keratin in 100 mMHNa_2PO_4 pH 9.0 Temperature 4	24.03234		Extensive
0.5 mg/mL of keratin in Ultrapure Water Temperature 37	25.78913	90%	Extensive
0.1 mg/mL of keratin in 100 mM HNa_2PO_4 pH 8.0 Temperature 37	26.13655		Severe
0.1 mg/mL of keratin in Ultrapure Water Temperature 25	27.38119		Severe
0.1 mg/mL of keratin in Ultrapure Water Temperature 37	29.76927		Severe
0.1 mg/mL of keratin in 10 mM HNa_2PO_4 pH 8.5 Temperature 25	30.65314		Severe
0.5 mg/mL of keratin in 100 mM HNa_2PO_4 pH 7.3 Temperature 37	32.02012		Severe
0.5 mg/mL of keratin in Ultrapure Water Temperature 25	33.09086		Severe
0.1 mg/mL of keratin in 100 mM HNa_2PO_4 pH 9.02 Temperature 25	37.4971		Severe

The lower the standard deviation suggests less aggregation while the higher the standard deviation suggests more aggregation. If the sample falls in the 0-25% quantile range there is suggestion of no aggregation, 25-50% quantile range there is suggestion of

mild aggregation, 50-75% quantile range there is suggestion of moderate aggregation, 75-90% quantile range there is suggestion of extensive aggregation, and 90-100% quantile range there is suggestion of severe aggregation. To see the standard deviations compared to each other in mean intensity size graphs as well as volume percent graphs all the bar graphs can be found in the Appendix A, B, and C.

Using the results presented above, a Levene's test was performed in order to better quantify the statistical significance of the data comparing different conditions. Levene's test reports a "p-value" which is compared to some threshold value. This comparison determines, in this case, whether all variances are equal or not. If the variances are equal, there is no significant difference between samples, whereas if the variances are not equal, the complexity of the samples is substantially different, indicating that one sample displays more aggregation. The Levene's test results are shown in Table 7 below. In Table 7, "All Buffers" or "All Waters" means that all keratin concentrations, all buffer concentrations, all salt concentrations, all pHs, and all temperatures were considered.

Table 7 Levene test p-values

Test	Test Peak	P-Value	Conclusion
All Buffer vs. All Water	Peak 1 Mean Intensity Size Standard Deviation	0.1115	All variances are equal
	Peak 2 Mean Intensity Size Standard Deviation	0.6373	All variances are equal
	Peak 1 Volume Percent Standard Deviation	0.3371	All variances are equal
	Peak 2 Volume Percent Standard Deviation	0.0204	Not all variances are equal
All Buffers at 0.5 mg/mL of Keratin vs. All Water at 0.5 mg/mL of Keratin	Peak 1 Mean Intensity Size Standard Deviation	<0.0001	Not all variances are equal
	Peak 2 Mean Intensity Size Standard Deviation	0.8408	All variances are equal
	Peak 1 Volume Percent Standard Deviation	0.0186	Not all variances are equal
	Peak 2 Volume Percent Standard Deviation	0.0158	Not all variances are equal
All Buffers at 0.1 mg/mL of Keratin vs. All Water at 0.1	Peak 1 Mean Intensity Size Standard Deviation	0.3860	All variances are equal
	Peak 2 Mean Intensity Size Standard Deviation	0.0931	All variances are equal
	Peak 1 Volume Percent Standard Deviation	0.4239	All variances are equal
	Peak 2 Volume Percent Standard Deviation	0.4868	All variances are equal

mg/mL of Keratin			
All 10 mM HNa_2PO_4 and 100 mM HNa_2PO_4 vs. all Water	Peak 1 Mean Intensity Size Standard Deviation	0.2297	All variances are equal
	Peak 2 Mean Intensity Size Standard Deviation	0.5733	All variances are equal
	Peak 1 Volume Percent Standard Deviation	0.7918	All variances are equal
	Peak 2 Volume Percent Standard Deviation	0.1258	All variances are equal
All 10/100 mM HNa_2PO_4/NaCl vs. all Water	Peak 1 Mean Intensity Size Standard Deviation	0.0248	Not all variances are equal
	Peak 2 Mean Intensity Size Standard Deviation	0.8744	All variances are equal
	Peak 1 Volume Percent Standard Deviation	0.0006	Not all variances are equal
	Peak 2 Volume Percent Standard Deviation	<0.0001	Not all variances are equal
All buffers at pH 7.4 vs. all water	Peak 1 Mean Intensity Size Standard Deviation	0.1370	All variances are equal
	Peak 2 Mean Intensity Size Standard Deviation	0.8326	All variances are equal
	Peak 1 Volume Percent Standard Deviation	0.4719	All variances are equal
	Peak 2 Volume Percent Standard Deviation	0.0132	Not all variances are equal
All buffers at pH 8 vs. all water	Peak 1 Mean Intensity Size Standard Deviation	0.0483	Not all variances are equal
	Peak 2 Mean Intensity Size Standard Deviation	0.3747	All variances are equal
	Peak 1 Volume Percent Standard Deviation	0.1142	All variances are equal
	Peak 2 Volume Percent Standard Deviation	0.0018	Not all variances are equal
All buffers at pH 8.5 vs. all water	Peak 1 Mean Intensity Size Standard Deviation	0.0971	All variances are equal
	Peak 2 Mean Intensity Size Standard Deviation	0.8425	All variances are equal
	Peak 1 Volume Percent Standard Deviation	0.2218	All variances are equal
	Peak 2 Volume Percent Standard Deviation	0.0088	Not all variances are equal
All buffers at pH 9 vs. all water	Peak 1 Mean Intensity Size Standard Deviation	0.5967	All variances are equal
	Peak 2 Mean Intensity Size Standard Deviation	0.5485	All variances are equal
	Peak 1 Volume Percent Standard Deviation	0.9321	All variances are equal
	Peak 2 Volume Percent Standard Deviation	0.3066	All variances are equal
All temperatures (4°C vs. 25°C vs. 37°C)	Peak 1 Mean Intensity Size Standard Deviation	0.2260	All variances are equal
	Peak 2 Mean Intensity Size Standard Deviation	0.0027	All variances are equal
	Peak 1 Volume Percent Standard Deviation	0.4131	All variances are equal
	Peak 2 Volume Percent Standard Deviation	0.1274	All variances are equal
All buffers at keratin concentration 0.1 mg/mL vs. all buffers at keratin concentration 0.5 mg/mL	Peak 1 Mean Intensity Size Standard Deviation	0.7698	All variances are equal
	Peak 2 Mean Intensity Size Standard Deviation	0.3462	All variances are equal
	Peak 1 Volume Percent Standard Deviation	0.0870	All variances are equal
	Peak 2 Volume Percent Standard Deviation	0.0680	All variances are equal
All 10 mM HNa_2PO_4 vs. all 100 mM HNa_2PO_4	Peak 1 Mean Intensity Size Standard Deviation	0.5793	All variances are equal
	Peak 2 Mean Intensity Size Standard Deviation	0.0398	Not all variances are equal
	Peak 1 Volume Percent Standard Deviation	0.0013	Not all variances are equal
	Peak 2 Volume Percent Standard Deviation	0.0008	Not all variances are equal
All 10 mM HNa_2PO_4 vs. all 10/100 mM HNa_2PO_4/NaCl	Peak 1 Mean Intensity Size Standard Deviation	0.0304	Not all variances are equal
	Peak 2 Mean Intensity Size Standard Deviation	0.1108	All variances are equal
	Peak 1 Volume Percent Standard Deviation	0.0763	All variances are equal
	Peak 2 Volume Percent Standard Deviation	0.0465	Not all variances are equal

2.4 DISCUSSION

As mentioned in the introduction, dynamic light scattering measures the hydrodynamic diameter of a sphere. Keratin is not a sphere, it is a thin rod as shown in Figure 1.3, which is made from two monomers that are bound together in a protein dimer complex. Steinert et al. performed an experiment and found the length of this keratin dimeric complex to be 46 nm and the diameter to be 5.5 nm [29]. Using the Stokes-Einstein equation mentioned in Section 1.7.1, Santos et al. suggest multiple correction factors to the equation to account for a rod. The newest correction factor by Berne and Pecora was chosen to calculate the theoretical rod length using the Stokes-Einstein equation. Where L is the rod length, a is the radius of the rod, and b is the half the rod's length [21].

$$D = \frac{kT}{6\pi n b'}\left(1 - \frac{a^2}{b^2}\right)^{-\frac{1}{2}} \quad \text{Eq 2.1}$$

$$b' = \frac{L}{2} \quad \text{Eq 2.2}$$

Solving for the equation,

$$D = \frac{kT}{6\pi n R_{sphere}} = \frac{kT}{6\pi n b'}\left(1 - \frac{a^2}{b^2}\right)^{-\frac{1}{2}} \quad \text{Eq 2.3}$$

$$\frac{1}{R_{sphere}} = \frac{1}{b'}\left(1 - \frac{a^2}{b^2}\right)^{-\frac{1}{2}} \quad \text{Eq 2.4}$$

Using literature's dimensions of keratin,

$$\frac{1}{R_{sphere}} = \frac{1}{23.5\ nm}\left(1 - \frac{2.75\ nm^2}{23.5\ nm^2}\right)^{-\frac{1}{2}} \quad \text{Eq 2.5}$$

$$\frac{1}{R_{sphere}} = 0.043\ nm \quad \text{Eq 2.6}$$

$$R_{sphere} = 23.3\ nm\ and\ D_{Sphere} = 46.7\ nm \quad \text{Eq 2.7}$$

Using the equations above, a dimeric keratin rod would appear to have a hydrodynamic diameter of about 46.7 nm in the DLS. Steinert et al. found that the rod without the head and tail regions is 46 nm [29]. In our experiments, peak 1 mean intensity size output ranges from 20-40nm. As discussed earlier, peak 1 mean intensity size refers to the smaller diameter of the instrument's software output; therefore, this peak in general should be associated with keratin dimers (i.e. keratin nanomaterial). Our measurements are smaller than 46.7 nm, probably because the rod is not always rotating around its geometric center (i.e. maximum apparent hydrodynamic diameter) and instead detected at different angles in front of the laser, thereby giving a slightly smaller apparent radius.

2.4.1 Does pH affect aggregation? The average pH of the human body is 7.4. The isoelectric point (pI) of keratin is 5.3 [30]. The regions being tested, pH 7.4-9.0, are consistently above the isoelectric point (pH's below the pI could not be tested because keratin precipitates below pH 7) so keratin has a net negative charge and is soluble at all values of pH. If keratin were tested around the isoelectric point, theoretically, there would be a lot of aggregation due to hydrophobic and Van der Waals forces. Also, keratin is insoluble at acidic pH and would precipitate out of solution.

As shown in the statistics data (Table 7), when comparing all the buffers at a different pH to water only, the standard deviation of pH 8 peak 1 mean intensity size stood out as not having equal variances. All the other conditions have equal variances, suggesting that pH does not have an effect on aggregation under these conditions. It is not conclusive why pH 8 would stand out from the other pH values.

As shown in the graphed data in Appendix A, B, and C, in general the volume percent did not change significantly between runs, which demonstrates lack of aggregation especially compared to water with the higher keratin concentration. There were, however, more runs with a larger standard deviation at the lower keratin concentration.

When averaging every run regardless of the keratin concentration, buffer concentration, buffer, and temperature, the average peak 1 mean intensity size (d.nm) is 28 nm for pH 7.4, 29 nm for pH 8.0, 30 nm for pH 8.5, 30 nm for pH 9, and 34 nm for Ultrapure water. Statistical analysis of these data suggests there is no difference in the size of the keratin dimer when the pH is altered in the different buffer solutions.

2.4.2 Does temperature affect aggregation? The average temperature of the human body is 37°C (98.6°F). Temperature 25°C (77°F) is on average, room temperature, and 4°C (39.2°F) is on average, refrigerator temperature. As shown in the statistics data (Table 7), when comparing all the temperatures to each other, all have equal variances. This means that there is no difference in aggregation behavior when changing temperatures.

As shown in the graphed data in the Appendix B, in general, the mean intensity size and volume percent did not vary significantly between runs. The volume percent appears to have larger standard deviations at 4°C compared to 25°C and 37°C.

When averaging every run regardless of the keratin concentration, buffer concentration, buffer, and pH, the peak 1 mean intensity size is 30 nm for temperature 4°C, 30 nm for temperature 25°C, and 29 nm for temperature 37°C. Therefore, temperature does not appear to effect the size of keratin nanomaterials in these solutions.

2.4.3 Does buffer concentration affect aggregation? Aebi et al. performed a study that showed keratins "unravel" in 1-10 mM HNa_2PO_4 at pH 7.5. The authors further demonstrated that this unraveling phenomenon occurred to different extents at different buffer concentrations. If the keratin is unraveled then theoretically there would be less aggregation happening due to phosphate "buffering" the ionic charges [27].

As shown in the statistics data (Table 7), when comparing 10 mM HNa_2PO_4 to 100 mM HNa_2PO_4 the standard deviation of peak 1 mean intensity size has equal variances; however, peak 1 volume percent standard deviation does not. This means the samples are not different when it comes to the size of the dimer in the system. However, the samples are different when it comes to the amount of aggregation in each system. The graphed data (Appendix B), supports this conclusion.

When averaging every run regardless of the keratin concentration, pH, and temperature, the average peak 1 mean intensity size (d.nm) is 30nm for 10 mM HNa_2PO_4, 30 nm for 100 mM HNa_2PO_4, and 34 nm for Ultrapure water. The sizes are statistically similar with regards to an increase in concentration, suggesting that buffer concentration does not appear to have an effect on keratin nanomaterial size.

2.4.4 Does salt affect aggregation? As discussed in the introduction, keratin monomers complex with each other by a variety of mechanisms including disulfide and ionic bonds. Aggregates form primarily through ionic bonds, but not all proteins aggregate to the same degree due to their complex tertiary structure. When NaCl is added to the solution, it should have the effect of occupying these ionic sites and reducing aggregation. Chan and Chen state that for a solution of 100 mM NaCl, the NaCl helps the proteins

remain solubilized. If a lot of NaCl is added to the solution, the protein will not denature because it would not be thermodynamically favorable as salt stabilizes the proteins, which also prevents aggregation [31].

As shown in the statistics data (Table 7), when comparing the buffer solution with and without salt, the standard deviation of peak 1 mean intensity size did not have equal variances, suggesting that the sample acts differently in both cases. The sample also did not have equal variances when comparing peak 1 mean intensity size standard deviation of the buffer concentration plus salt to water, again suggesting the sample acts differently in both cases.

As shown in the graphed data in Appendix B, in general the volume percent did not change much from run to run, which demonstrated sample stability, especially compared to water. Also, when comparing the addition of 100mM of NaCl to 10mM HNa_2PO_4, the sizes are comparable.

When averaging every run regardless of the keratin concentration, buffer concentration, pH, and temperature, the average peak 1 mean intensity size (d.nm) is 30 nm for 10 mM HNa_2PO_4, 28 nm for 10/100 mM HNa_2PO_4/NaCl, and 34 nm for Ultrapure water. Based on these data, it not conclusive to say there is a difference in the size of the dimer when NaCl is added to the buffer solution.

2.4.5 Does keratin concentration affect aggregation? Theoretically, a higher keratin concentration leads to a higher collision rate among dissolved molecules, which would result in more aggregation.

As shown in the statistics data (Table 7), when comparing all the buffers at keratin concentration 0.1 mg/mL to all the buffers at keratin concentration 0.5 mg/mL, all of the variances are equal, meaning that aggregation does not change based on concentration.

As shown in the graphed data in Appendix C, peak 1 mean intensity size shows that all the sizes are comparable at the two levels of keratin concentration. However, the peak 1 mean intensity size of keratin concentration at 0.5 mg/mL is slightly larger than keratin concentration 0.1 mg/mL at temperature 37°C. This suggests that while keratin concentration alone might not have an effect on aggregation, when combined with another environmental condition it may.

When averaging every run regardless of the buffer concentration, addition of salt, pH, and temperature, the average peak 1 mean intensity size (d.nm) is 29 nm for 0.1 mg/mL and 30 nm for 0.5 mg/mL. Again, these data suggest it is not conclusive to say there is a difference in the size of the dimer when the keratin concentration alone is changed.

2.4.6 Does water affect aggregation? As discussed earlier, the buffers affect the ionic charges of the keratin protein and "buffer" them from interacting with each other. With this being said, when there is no buffer in the system (i.e. pure water), there is nothing to get in between one keratin protein and another. This means that theoretically they could bind to each other and form aggregates.

As shown in the statistics data (Table 7), all buffers compared to all water samples have equal variances. However, when comparing just 0.5 mg/mL buffers to 0.5 mg/mL waters then peak 1 mean intensity size and peak 1 volume percent have unequal variances.

This is not conclusive because 0.5 mg/mL keratin in buffer solution has a sample size of 36, while water has a sample size of 3.

As shown in the graphed data in Appendix A, B, and C, water has a higher standard deviation than any buffer for the volume intensity peak 1 and 2 area percentages. Temperature 4°C peak 1 volume percent at keratin concentration 0.5 mg/mL has a very low standard deviation which is comparable to most buffer solutions. However, it is not clear why this is the case. In all other conditions, water has a much larger standard deviation. As shown in Table 8 below, keratin in water gives rise to a range of peak 1 mean intensity sizes. It is difficult to say which size or volume percent is correct when each appears more than once. Importantly, the range of sizes leads to large standard deviations as mentioned above, which suggests a high degree of aggregation.

Table 8 Seven runs for 0.5 mg/mL of keratin in Ultrapure water at temperature 37°C. This is a representation of the water runs.

Peak 1 Mean Intensity Size (d.nm)	Peak 1 Volume Percent (%)
31.67	99.4
38.11	99.4
30.07	99.1
34.77	43.7
32.3	49.5
32.24	99.4
38.37	99.4

When averaging every run regardless of the keratin concentration, buffer concentration, pH, and temperature, the average peak 1 mean intensity size (d.nm) is 29 nm for all buffers and 34 nm for water. There is about a 5 nm difference. However, this difference was not found to be statistically significant, largely due to the standard deviation of the values for water solutions.

While averaging 72 sample conditions (i.e. all buffers) to compare to all Ultrapure water (6 total samples), it is not surprising that statistical analysis did not identify a significant difference. Still, the aforementioned data suggests water promotes aggregation based on the higher standard deviations and the range of sizes and volume percentages.

As discussed earlier, peak 2 mean intensity size refers to the larger diameter particles; therefore, this peak can be considered aggregates of peak 1. Peak 2 mean intensity size ranged from 100-600nm. Based on the four assembly models discussed in the introduction, tetramers can range from 50-100nm. Peak 2 volume percent should then represent aggregates larger than two dimers.

In general, the size in diameter graphs show that buffer 10 mM HNa_2PO_4 pH 9 at temperature 4°C has a much higher standard deviation than the other pH's as well as a mean size that is also 200 nm larger than the rest. Buffer 10/100 mM HNa_2PO_4/NaCl pH 8 also has a much higher standard deviation than the rest of the pH's as well as a mean size that is about 100 nm larger than the rest. All the sizes are comparable at the two levels of keratin concentration. However, the diameter of keratin at a keratin concentration at 0.5 mg/mL is slight larger than the diameter at 0.1 mg/mL. The volume percent graphs show that only randomly does one pH tend to have a much larger standard deviation than the rest. Temperature 25°C shows less aggregation than the other two temperatures. Ultrapure water has a higher standard deviation than any other buffer at temperature 37°C and keratin concentration of 0.5 mg/mL at temperature 4°C. The pH and temperature alone do not have an effect on aggregation, but possibly might when combined with the type of buffer.

CHAPTER 3 –CONCLUSIONS AND FUTURE WORK

Not surprisingly, this study has shown that keratin nanomaterials in un-buffered solution aggregate to a greater extent than certain buffered systems. However, it is surprising that most of the literature describes keratin purification methods and keratin biomaterial production methods that employ pure water. Importantly, all of the changes to buffer concentration, keratin concentration, pH, and temperature were shown to have little effect on aggregation behavior. This is important as it defines a wide working range for buffered systems in terms of variable of pH, temperature, keratin concentration, and buffer concentration, at least for the buffers tested. In order to draw the conclusion that these slight differences, in combination with each other, effect aggregation, more experiments are necessary.

From a processing standpoint, the limited differences in dimer and aggregate size over a large range of environmental conditions mean that the system is relatively easy to control. The only factor that should be considered is using water versus a buffered system. When using a buffer system, it does not matter if the keratin concentration is between 0.1 mg/mL and 0.5 mg/mL, the pH is between 7.4 and 9, the buffer has added NaCl, or the temperature is between 4-37°C. Water, however, is used in labs around the world for processing keratin to eliminate salts and toxic chemicals used during extraction. Therefore, the results of the present study show that current keratin purification methods can lead to high levels of aggregation, which in turn will effect certain methods of separation (e.g. ultrafiltration).

In order to be more confident in the conclusions above, further experimentation should be performed. The use of circular dichroism would be useful to see if the

environment is actually playing a role in altering the secondary structure of the keratin nanomaterial, which cannot be determined by DLS. The experiments listed below should be performed:

- Test 1M HNa_2PO_4 and 10M HNa_2PO_4 to see if increasing the buffer solution leads to no aggregation.
- Test a solution of 100 mM NaCl only, and compare to 1M of NaCl added to the current buffer solution to see if too much sodium chloride would stabilize the solution.
- Test 1/1 M of HNa_2PO_4/NaCl to complete the test matrix and have a better understanding of what high levels of buffer and salt combined would do.
- Test 10 mM of KH_2PO_4, 100 mM of KH_2PO_4, and 10/100 mM of KH_2PO_4/KCl to see the difference between potassium and sodium.
- Compare the effects of KCl and NaCl.

It is important to remember that while there is a large amount of keratin research in the literature, there are multiple types of keratin derived using several methods, from multiple sources. While there is enough evidence to support that all keratins are very similar, there is not enough evidence to report that they are exactly the same and behave the same under environmental conditions such as buffer composition and concentration, temperature and pH.

REFERENCES

[1] J. G. Rouse and M. E. Van Dyke, "A Review of Keratin-Based Biomaterials for Biomedical Applications," *Materials,* vol. 3, pp. 999-1014, 2010.

[2] R. C. Marshall, D. F. G. Orwin, and J. M. Gillespie, "Structure and Biochemistry of Mammalian Hard Keratin," *Electron Microsc. Rev.,* vol. 4, pp. 47-83, 1991.

[3] J. Schweizer, P. E. Bowden, P. A. Coulombe, L. Langbein, E. B. Lane, T. M. Magin*, et al.*, "New consensus nomenclature for mammalian keratins," *The Journal of cell biology,* vol. 174, pp. 169-174, 2006.

[4] B. Alberts, D. Bray, J. Lewis, M. Raff, K. Roberts, and J. D. Watson, *Molecular Biology of the Cell (3rd edn)* vol. 20. New York, NY: Garland Publishing, 1994.

[5] W. Crewther, L. Dowling, P. Steinert, and D. Parry, "Structure of intermediate filaments," *International Journal of Biological Macromolecules,* vol. 5, pp. 267-274, 1983.

[6] H. B. Chase, "Growth of the hair," *Physiological Reviews,* vol. 34, pp. 113-126, 1954.

[7] M. P. Philpott, M. R. Green, and T. Kealey, "Human hair growth in vitro," *Journal of cell science,* vol. 97, pp. 463-471, 1990.

[8] M. Feughelman, "A Two-Phase Structure for Keratin Fibers," *Textile Research Journal,* vol. 29, pp. 223-228, 1959.

[9] L. Pauling and R. B. Corey, "Compound helical configurations of polypeptide chains: structure of proteins of the α-keratin type," *Nature,* vol. 171, 1953.

[10] U. Aebi, M. Häner, J. Troncoso, R. Eichner, and A. Engel, "Unifying principles in intermediate filament (IF) structure and assembly," *Protoplasma,* vol. 145, pp. 73-81, 1988.

[11] H. H. Bragulla and D. G. Homberger, "Structure and functions of keratin proteins in simple, stratified, keratinized and cornified epithelia," *Journal of anatomy,* vol. 214, pp. 516-559, 2009.

[12] H. Herrmann, T. Wedig, R. M. Porter, E. B. Lane, and U. Aebi, "Characterization of early assembly intermediates of recombinant human keratins," *Journal of structural biology,* vol. 137, pp. 82-96, 2002.

[13] P. M. Steinert, "Analysis of the mechanism of assembly of mouse keratin 1/keratin 10 intermediate filaments in vitro suggests that intermediate filaments are built from multiple oligomeric units rather than a unique tetrameric building block," *Journal of structural biology,* vol. 107, pp. 175-188, 1991.

[14] P. Hill, H. Brantley, and M. Van Dyke, "Some properties of keratin biomaterials: kerateines," *Biomaterials,* vol. 31, pp. 585-93, Feb 2010.

[15] R. C. de Guzman, M. R. Merrill, J. R. Richter, R. I. Hamzi, O. K. Greengauz-Roberts, and M. E. Van Dyke, "Mechanical and biological properties of keratose biomaterials," *Biomaterials,* vol. 32, pp. 8205-17, Nov 2011.

[16] A. Nakamura, M. Arimoto, K. Takeuchi, and T. Fujii, "A rapid extraction procedure of human hair proteins and identification of phosphorylated species," *Biological & pharmaceutical bulletin,* vol. 25, pp. 569-572, 2002.

[17] S. Shin, A. Lee, S. Lee, K. Lee, J. Kwon, M. Y. Yoon*, et al.*, "Microwave-assisted extraction of human hair proteins," *Analytical biochemistry,* vol. 407, pp. 281-283, 2010.

[18] A. Franbourg, P. Hallegot, F. Baltenneck, C. Toutain, and F. Leroy, "Current research on ethnic hair," *J Am Acad Dermatol,* vol. 48, pp. S115-9, Jun 2003.

[19] P. Alexander, R. Hudson, and M. Fox, "The reaction of oxidizing agents with wool. 1. The division of cystine into two fractions of widely differing reactivities," *Biochemical Journal,* vol. 46, p. 27, 1950.

[20] M. Van Dyke, private communication, Dec. 2013.
[21] N. C. Santos and M. Castanho, "Teaching light scattering spectroscopy: the dimension and shape of tobacco mosaic virus," *Biophysical journal,* vol. 71, p. 1641, 1996.
[22] R. Pecora, "Dynamic light scattering measurement of nanometer particles in liquids," *Journal of nanoparticle research,* vol. 2, pp. 123-131, 2000.
[23] G. D. Phillies, "Quasielastic light scattering," *Analytical Chemistry,* vol. 62, pp. 1049A-1057A, 1990.
[24] Malvern Instruments, private communication, Oct. 2014.
[25] C. Sinn, "Dynamic light scattering by rodlike particles: examination of the vanadium (V)-oxide system," *The European Physical Journal B-Condensed Matter and Complex Systems,* vol. 7, pp. 599-605, 1999.
[26] J. M. Cassel, "Collagen aggregation phenomena," *Biopolymers,* vol. 4, pp. 989-997, 1966.
[27] U. Aebi, W. E. Fowler, P. Rew, and T.-T. Sun, "The fibrillar substructure of keratin filaments unraveled," *The Journal of cell biology,* vol. 97, pp. 1131-1143, 1983.
[28] O. H. Lowry, N. J. Rosebrough, A. L. Farr, and R. J. Randall, "Protein measurement with the Folin phenol reagent," *J biol Chem,* vol. 193, pp. 265-275, 1951.
[29] P. M. Steinert, L. N. Marekov, R. Fraser, and D. A. Parry, "Keratin intermediate filament structure: crosslinking studies yield quantitative information on molecular dimensions and mechanism of assembly," *Journal of molecular biology,* vol. 230, pp. 436-452, 1993.
[30] R. C. De Guzman, private communication, Aug. 2014.
[31] R. Chan and V. Chen, "The effects of electrolyte concentration and pH on protein aggregation and deposition: critical flux and constant flux membrane filtration," *Journal of Membrane Science,* vol. 185, pp. 177-192, 2001.

Appendix A Compare temperatures

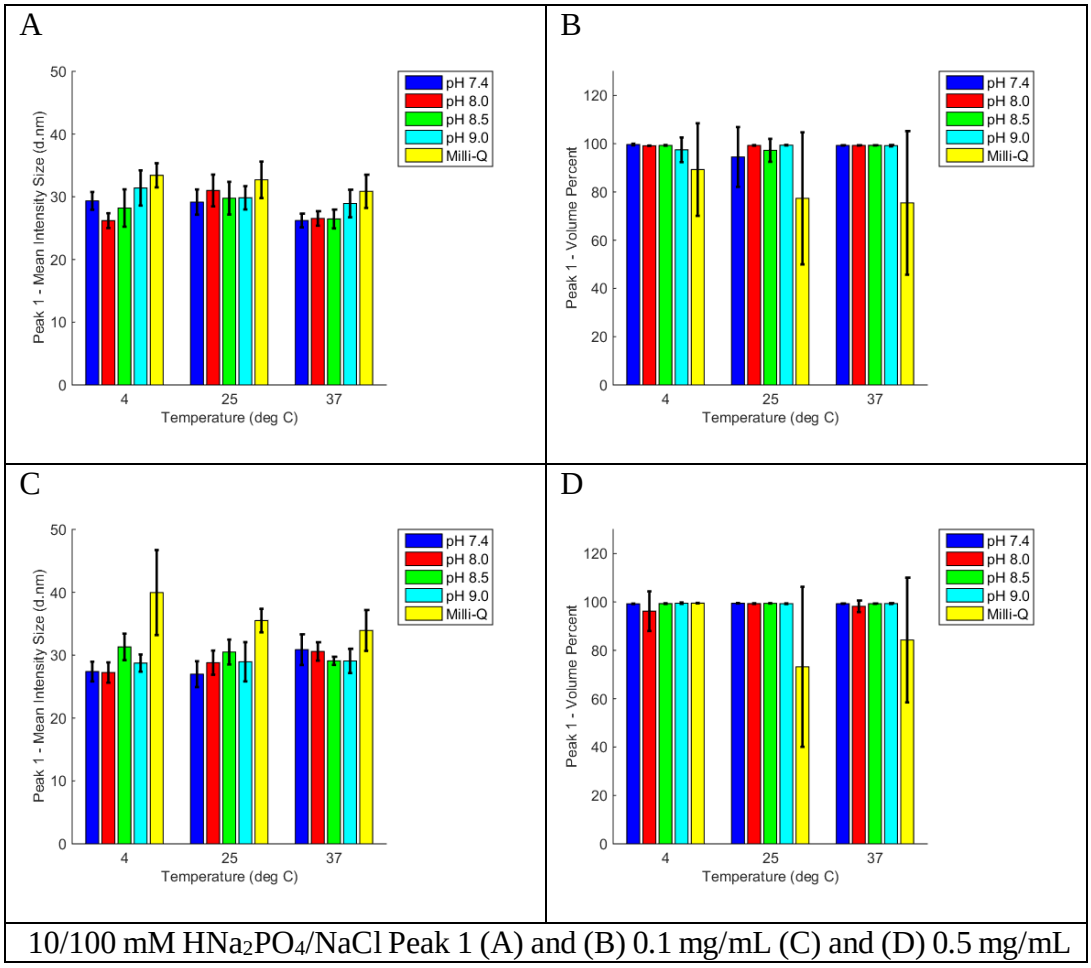

10/100 mM HNa_2PO_4/NaCl Peak 1 (A) and (B) 0.1 mg/mL (C) and (D) 0.5 mg/mL

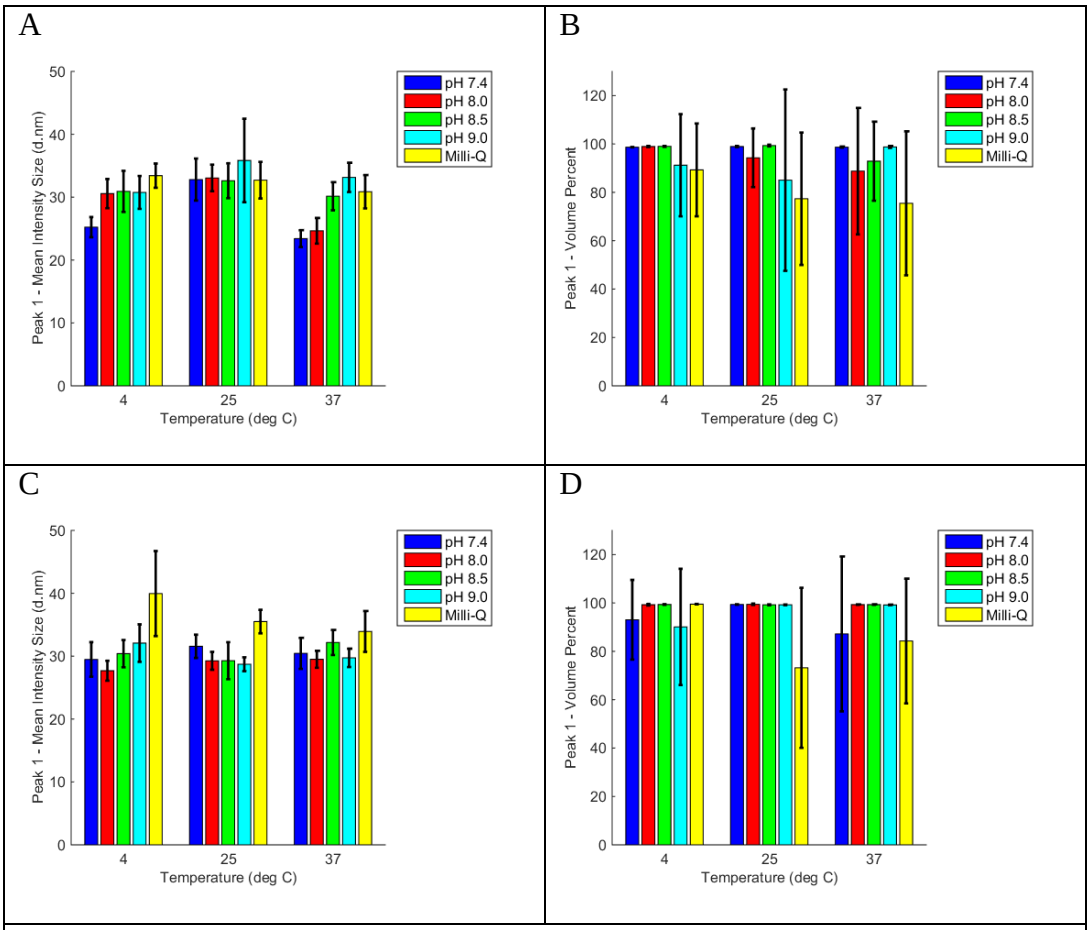

100 mM HNa_2PO_4 Peak 1 (A) and (B) 0.1 mg/mL (C) and (D) 0.5 mg/mL

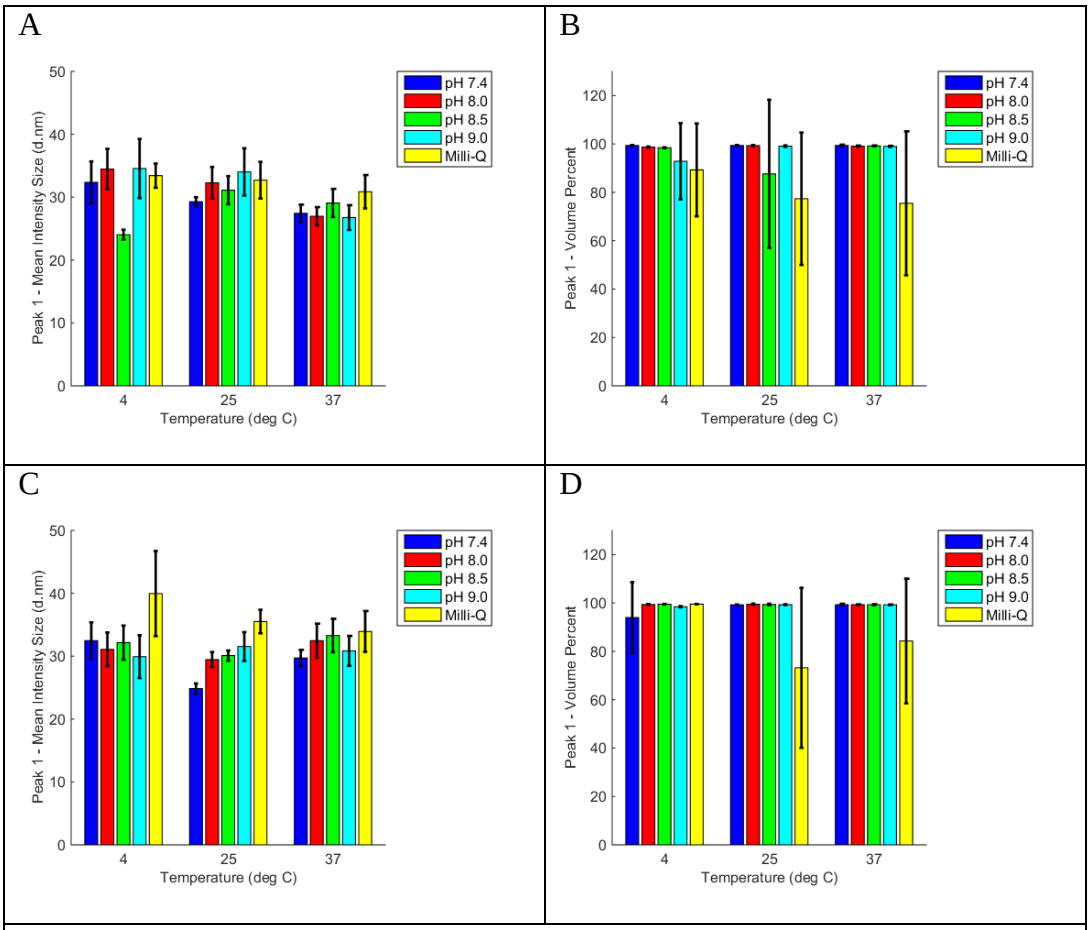

10 mM HNa_2PO_4 Peak 1 (A) and (B) 0.1 mg/mL (C) and (D) 0.5 mg/mL

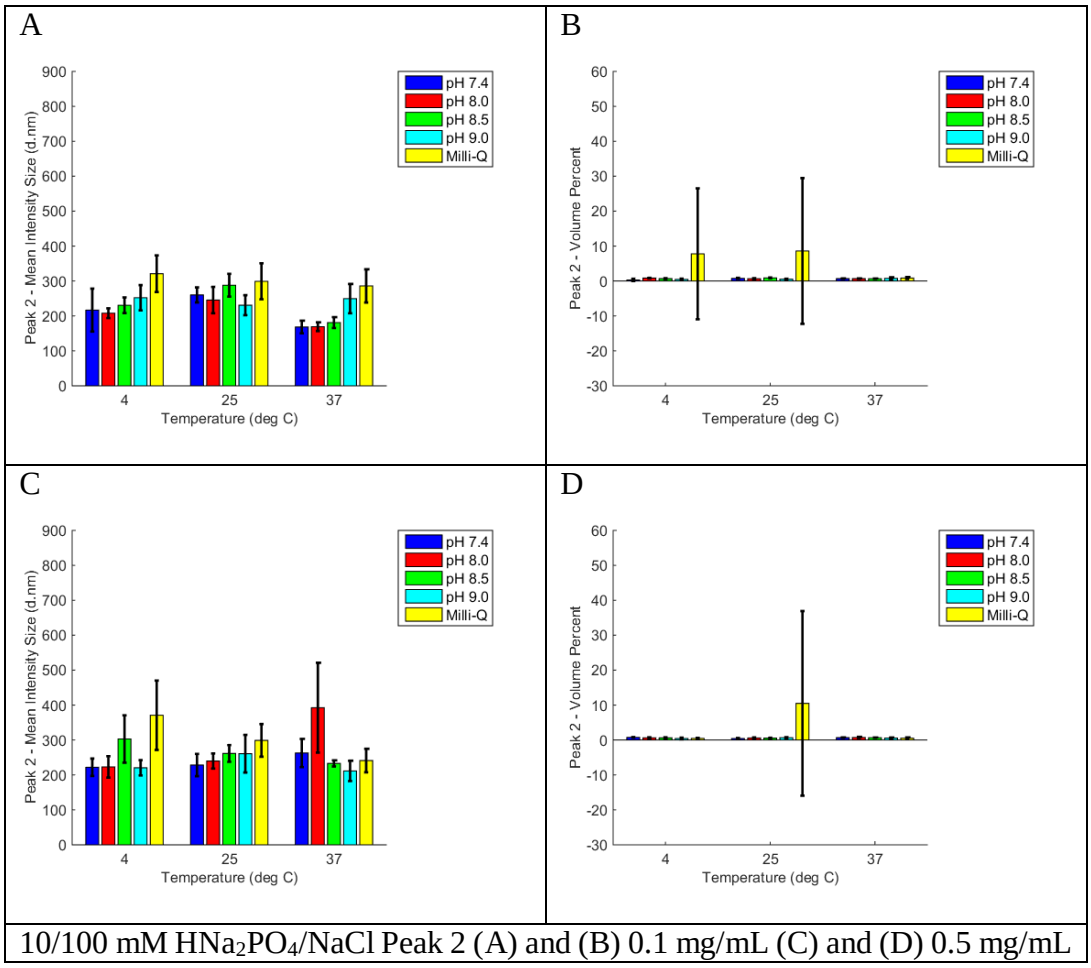

10/100 mM HNa_2PO_4/NaCl Peak 2 (A) and (B) 0.1 mg/mL (C) and (D) 0.5 mg/mL

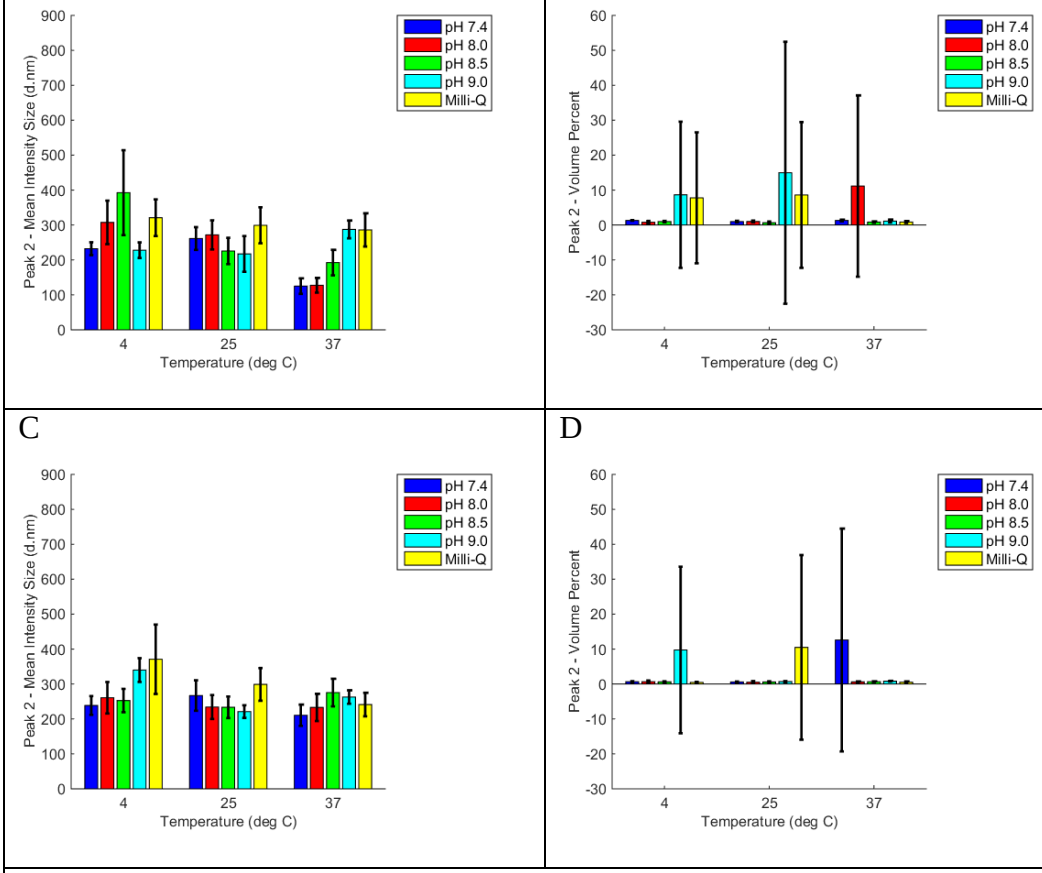

100 mM HNa_2PO_4 Peak 2 (A) and (B) 0.1 mg/mL (C) and (D) 0.5 mg/mL

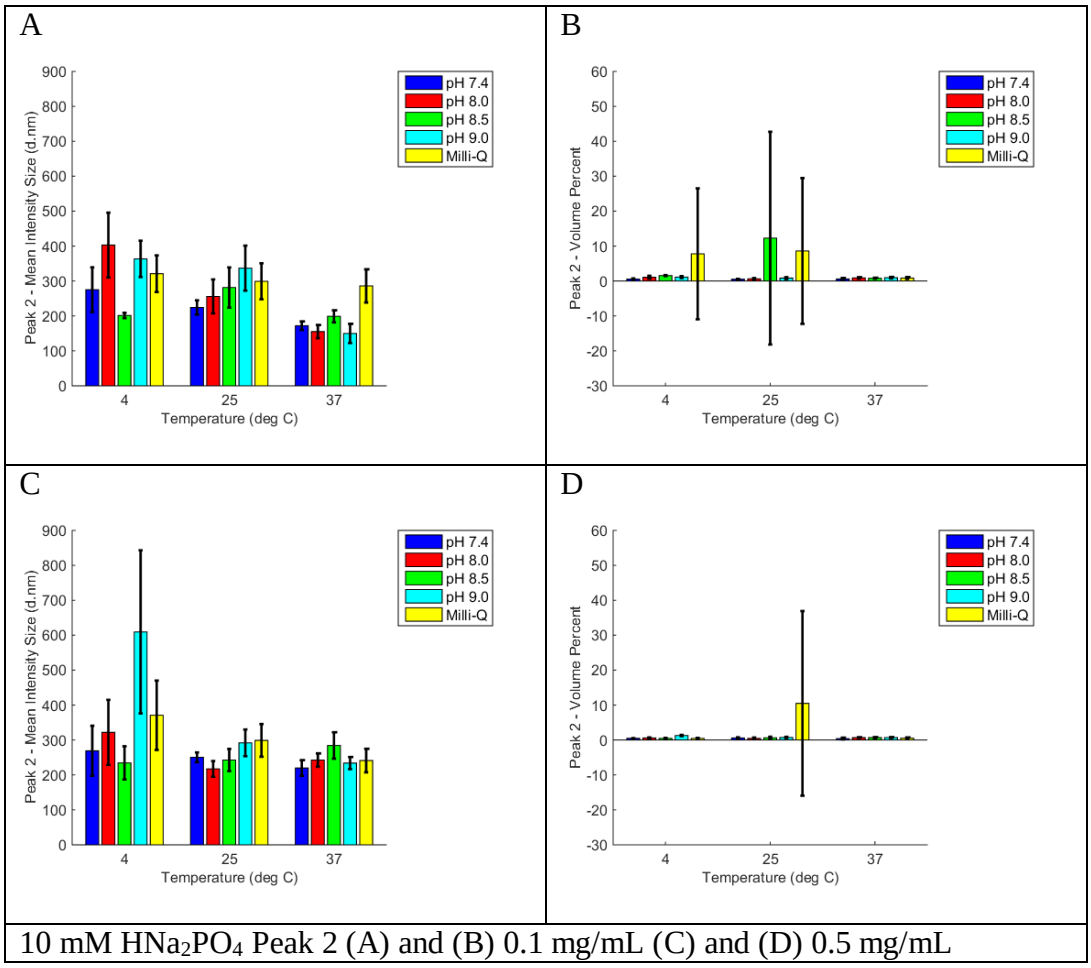

10 mM HNa_2PO_4 Peak 2 (A) and (B) 0.1 mg/mL (C) and (D) 0.5 mg/mL

Appendix B Compare buffers

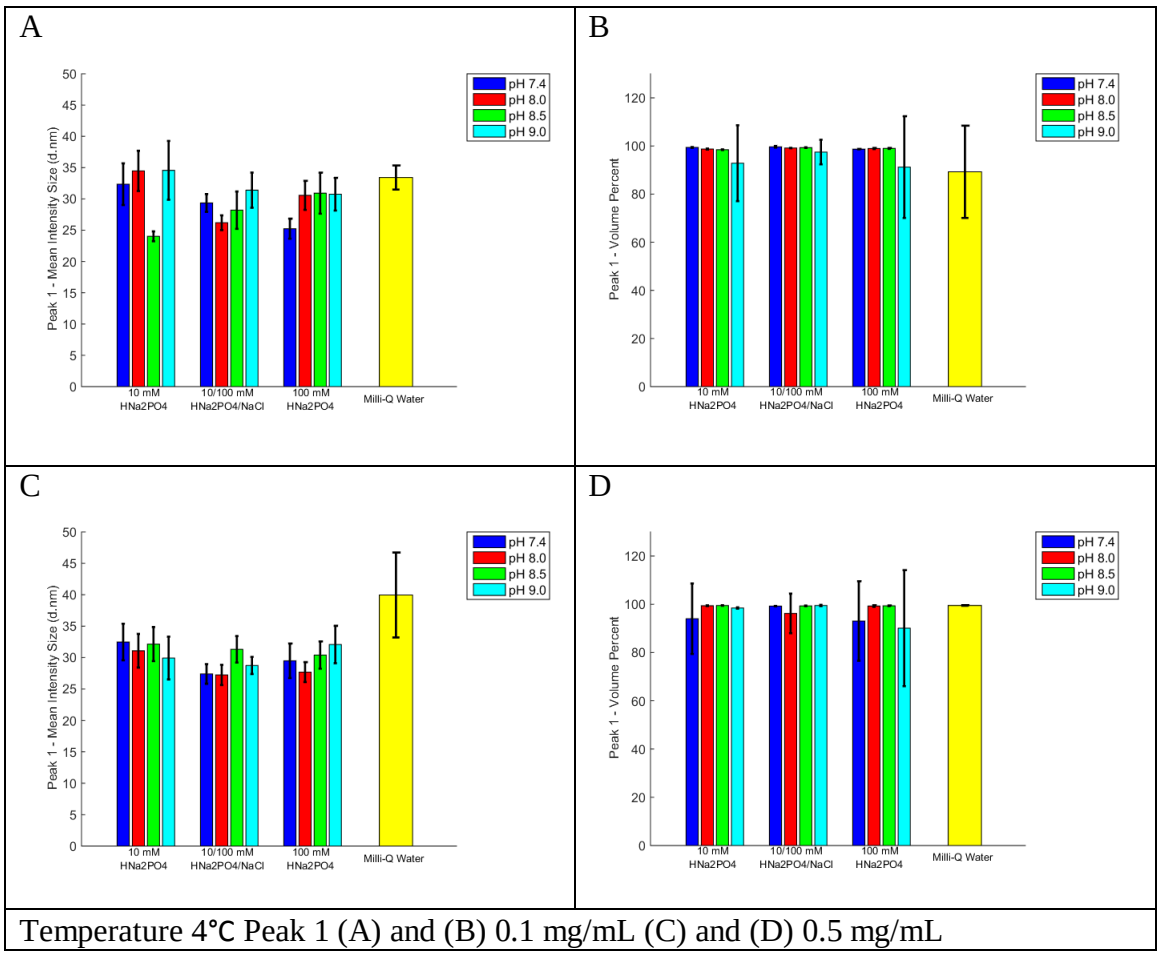

Temperature 4℃ Peak 1 (A) and (B) 0.1 mg/mL (C) and (D) 0.5 mg/mL

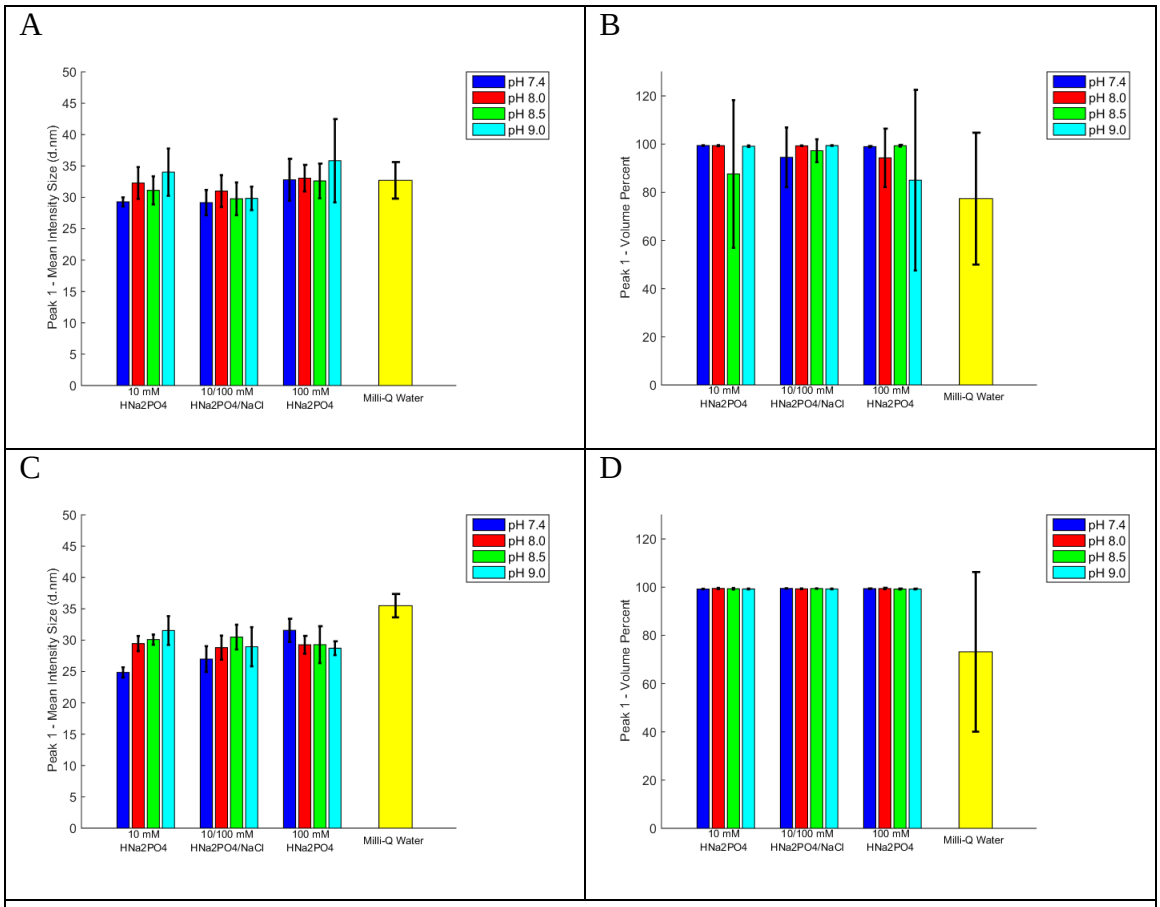

Temperature 25℃ Peak 1 (A) and (B) 0.1 mg/mL (C) and (D) 0.5 mg/mL

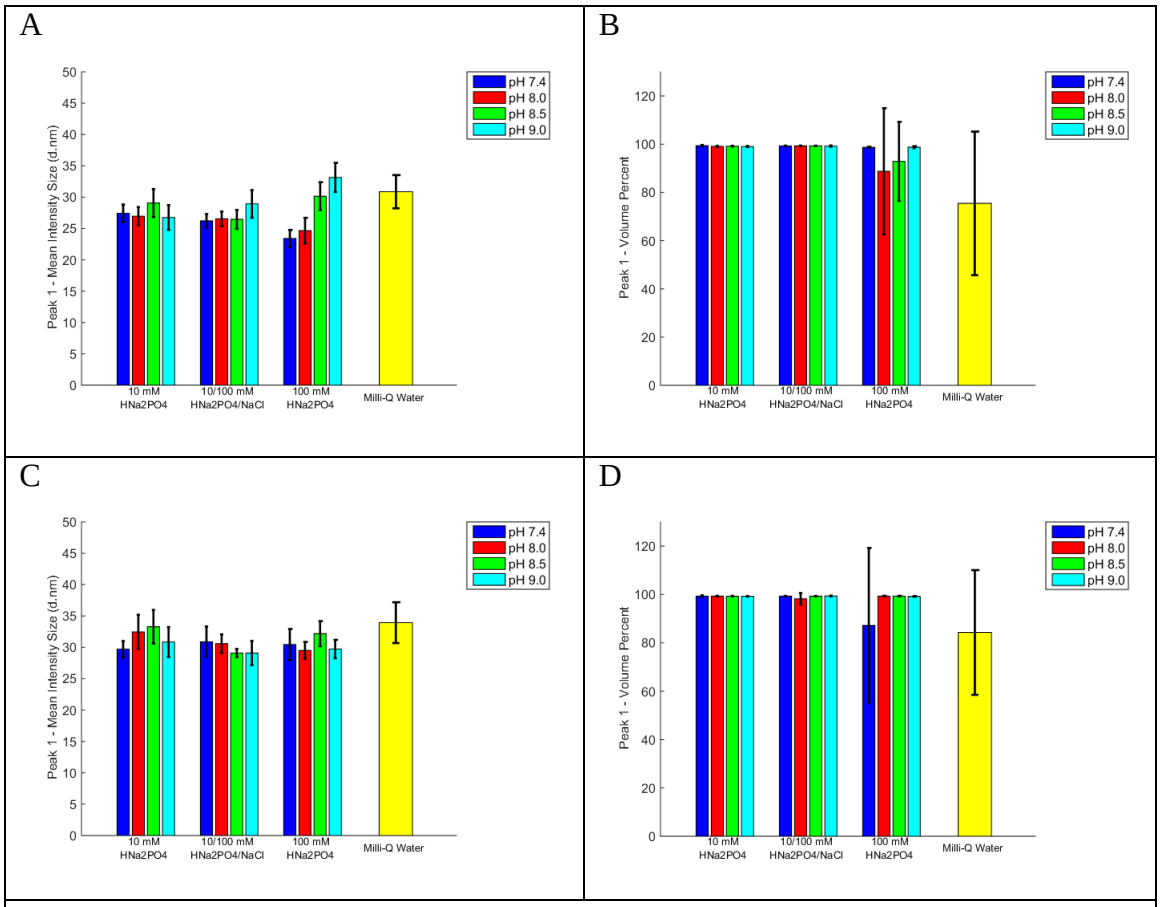

Temperature 37℃ Peak 1 (A) and (B) 0.1 mg/mL (C) and (D) 0.5 mg/mL

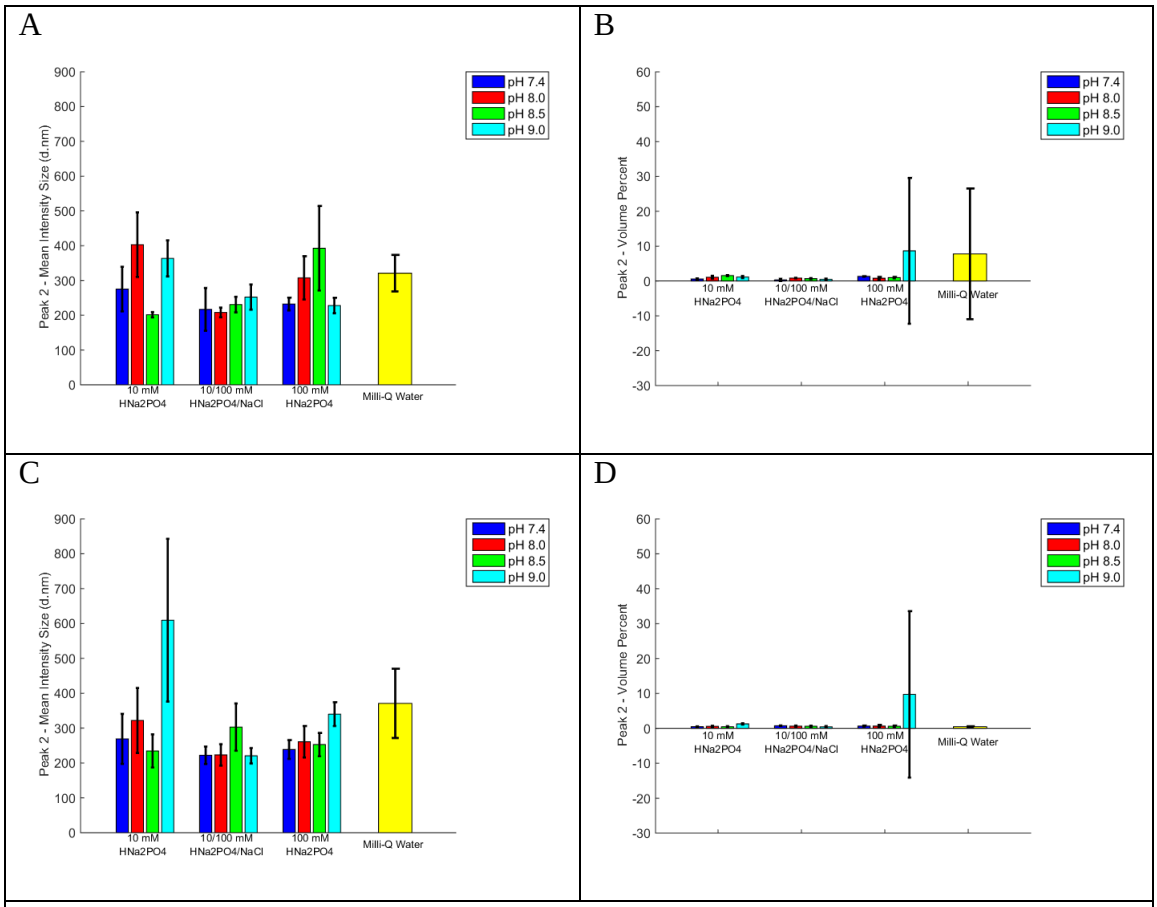

Temperature 4℃ Peak 2 (A) and (B) 0.1 mg/mL (C) and (D) 0.5 mg/mL

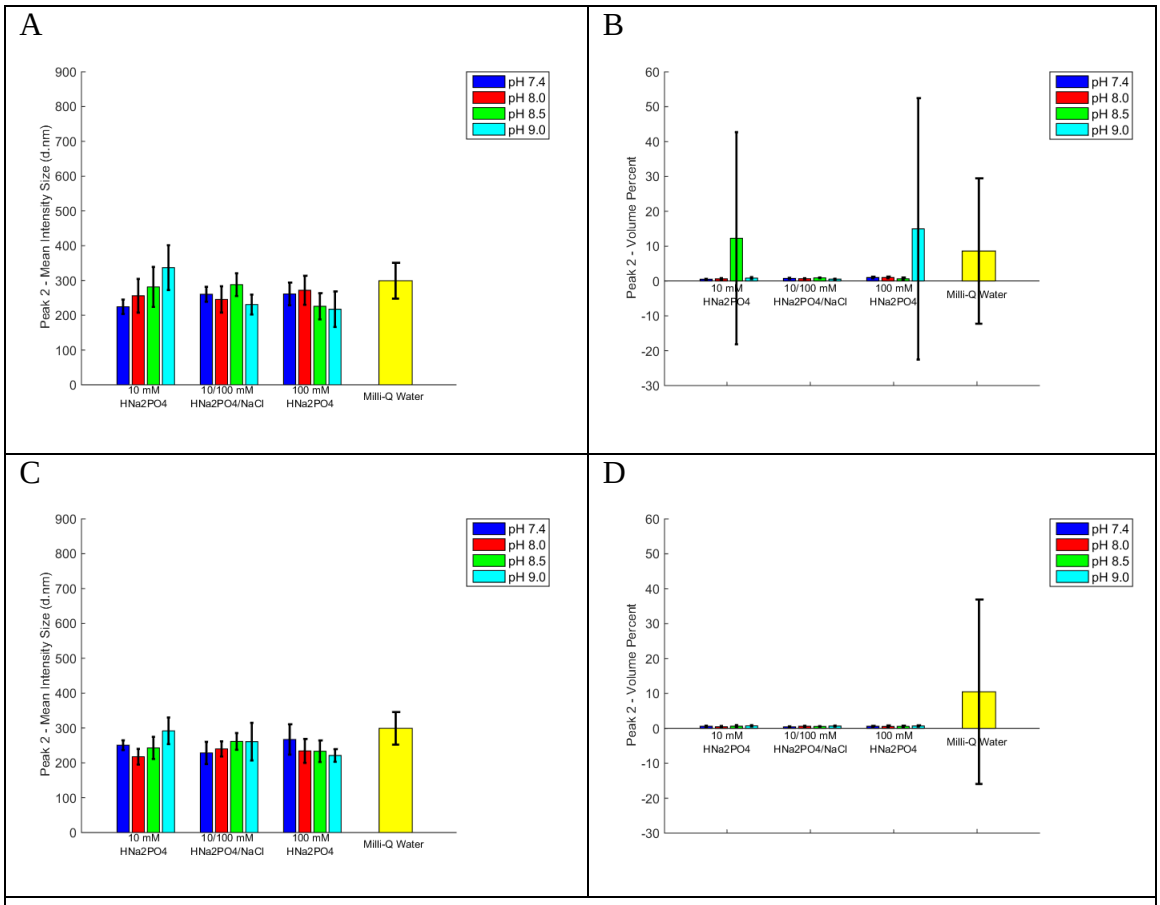

Temperature 25℃ Peak 2 (A) and (B) 0.1 mg/mL (C) and (D) 0.5 mg/mL

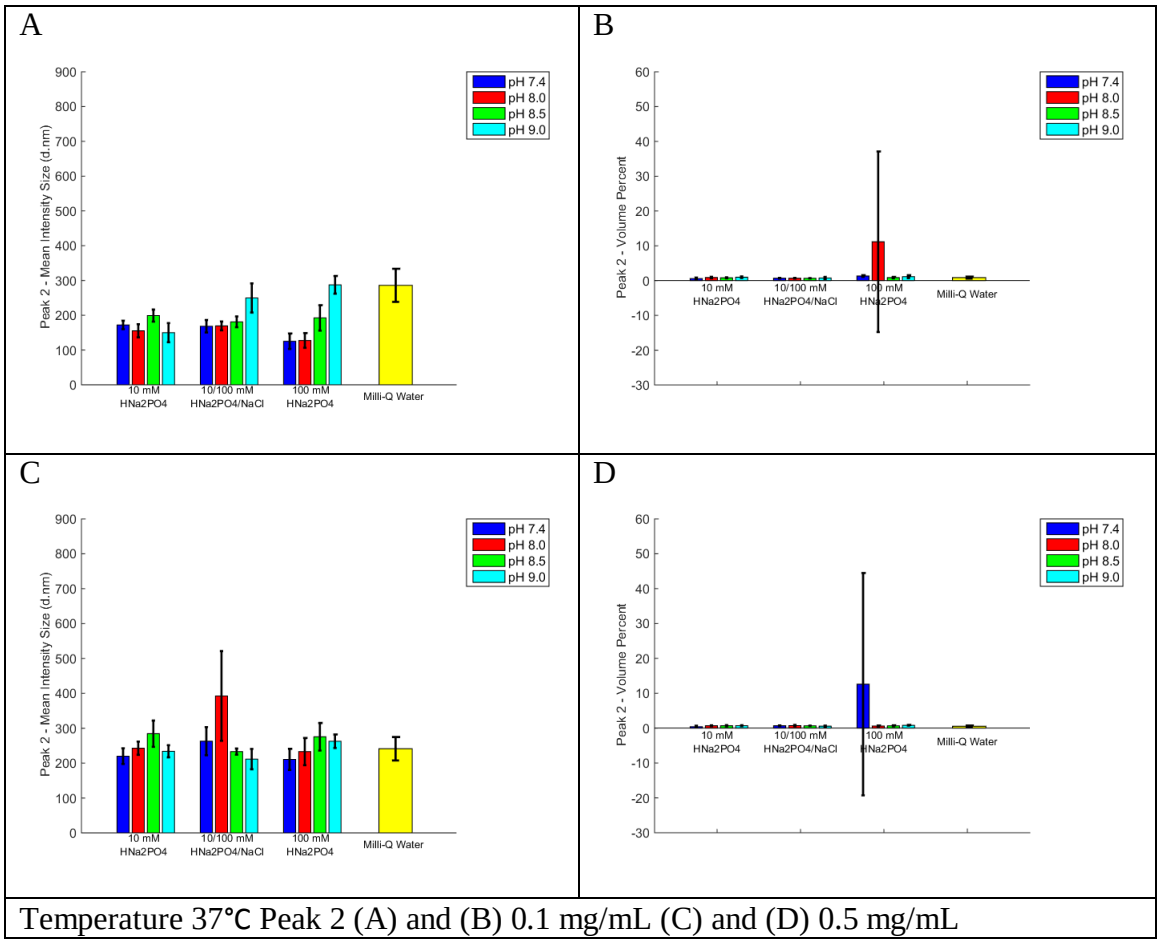

Temperature 37℃ Peak 2 (A) and (B) 0.1 mg/mL (C) and (D) 0.5 mg/mL

Appendix C Compare keratin concentration

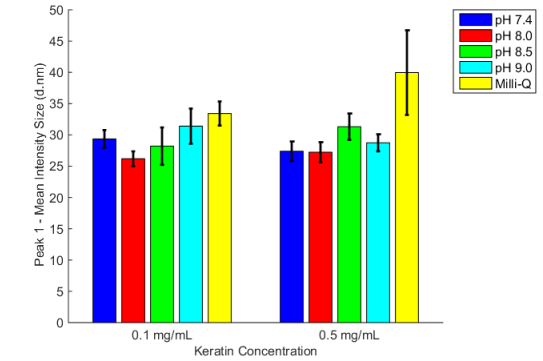

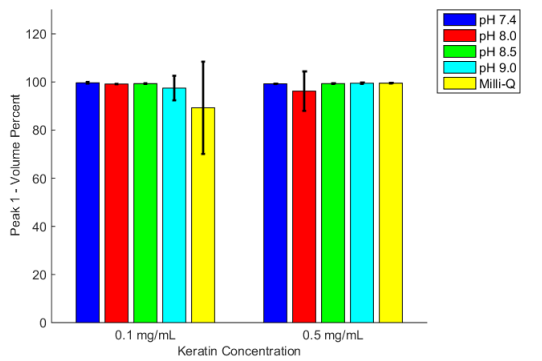

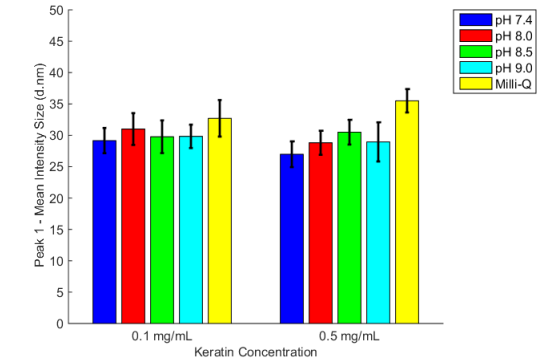

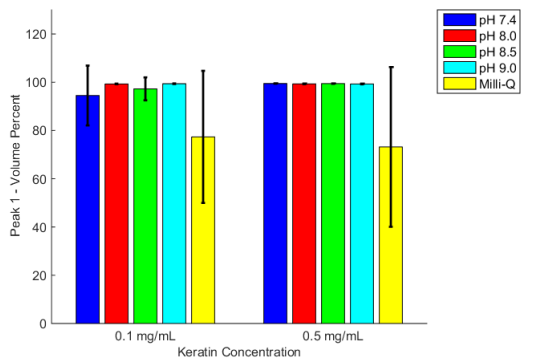

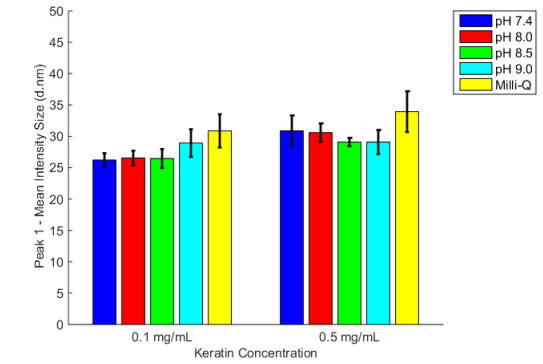

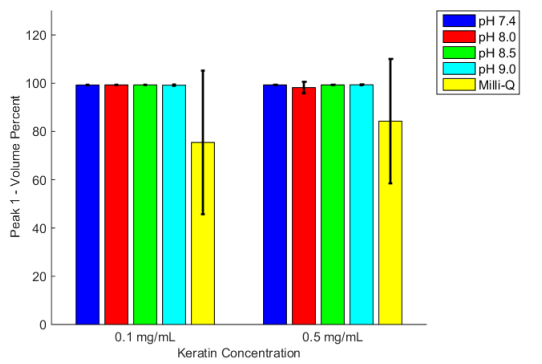

10/100 mM HNa_2PO_4/NaCl Peak 1 (A) and (B) Temperature 4°C (C) and (D) Temperature 25°C (E) and (F) Temperature 37°C

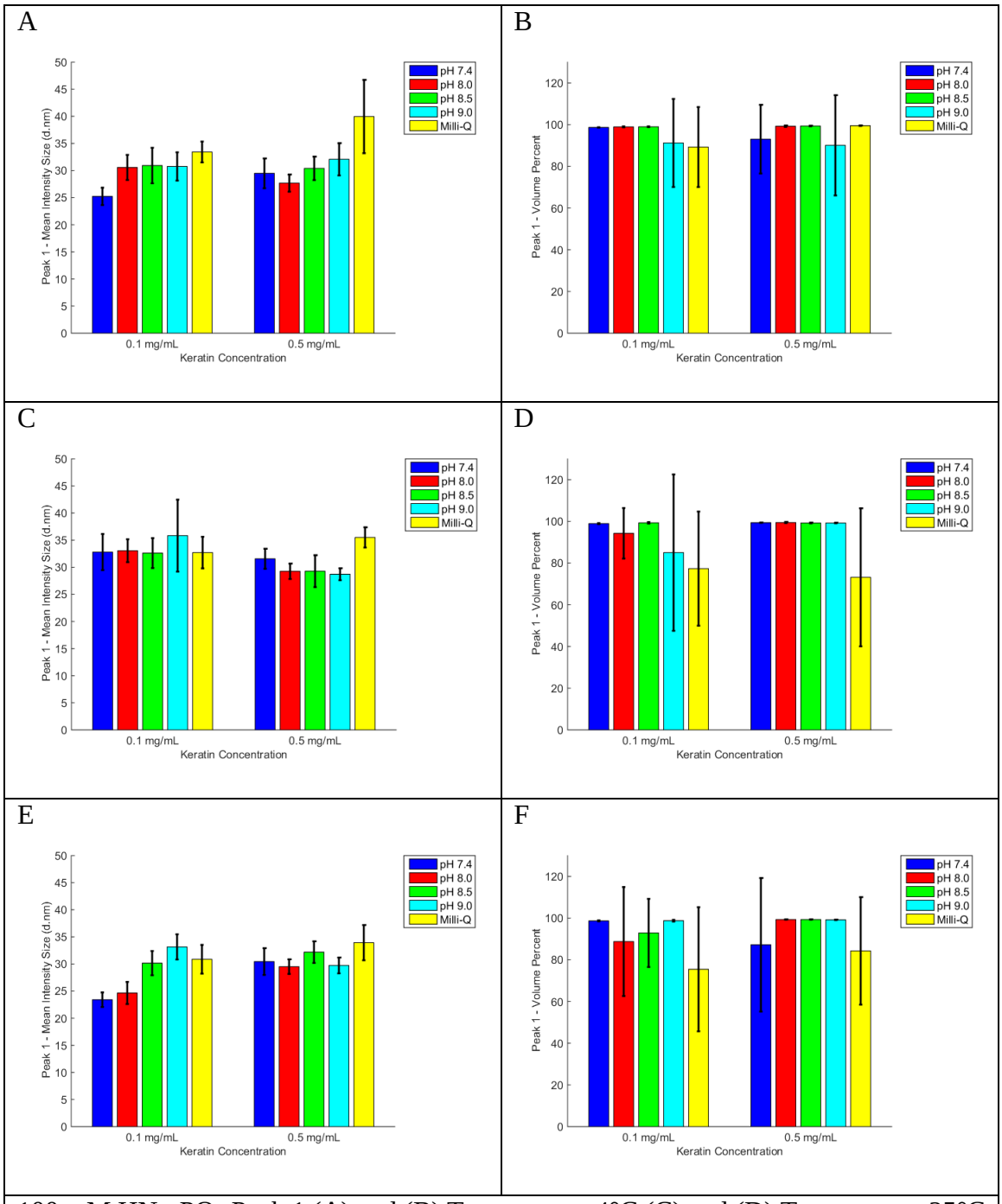

100 mM HNa_2PO_4 Peak 1 (A) and (B) Temperature 4°C (C) and (D) Temperature 25°C (E) and (F) Temperature 37°C

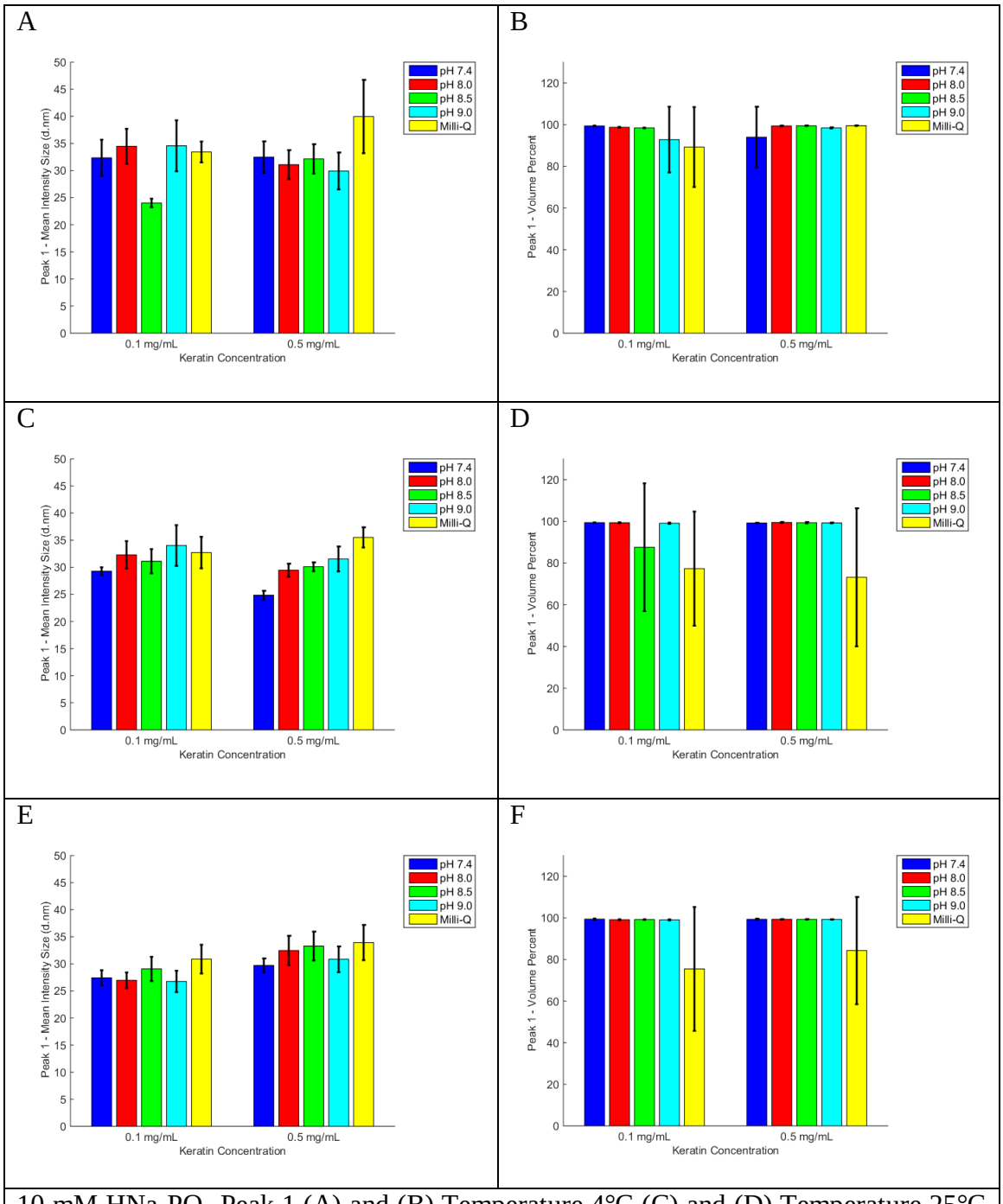

10 mM HNa_2PO_4 Peak 1 (A) and (B) Temperature 4°C (C) and (D) Temperature 25°C (E) and (F) Temperature 37°C

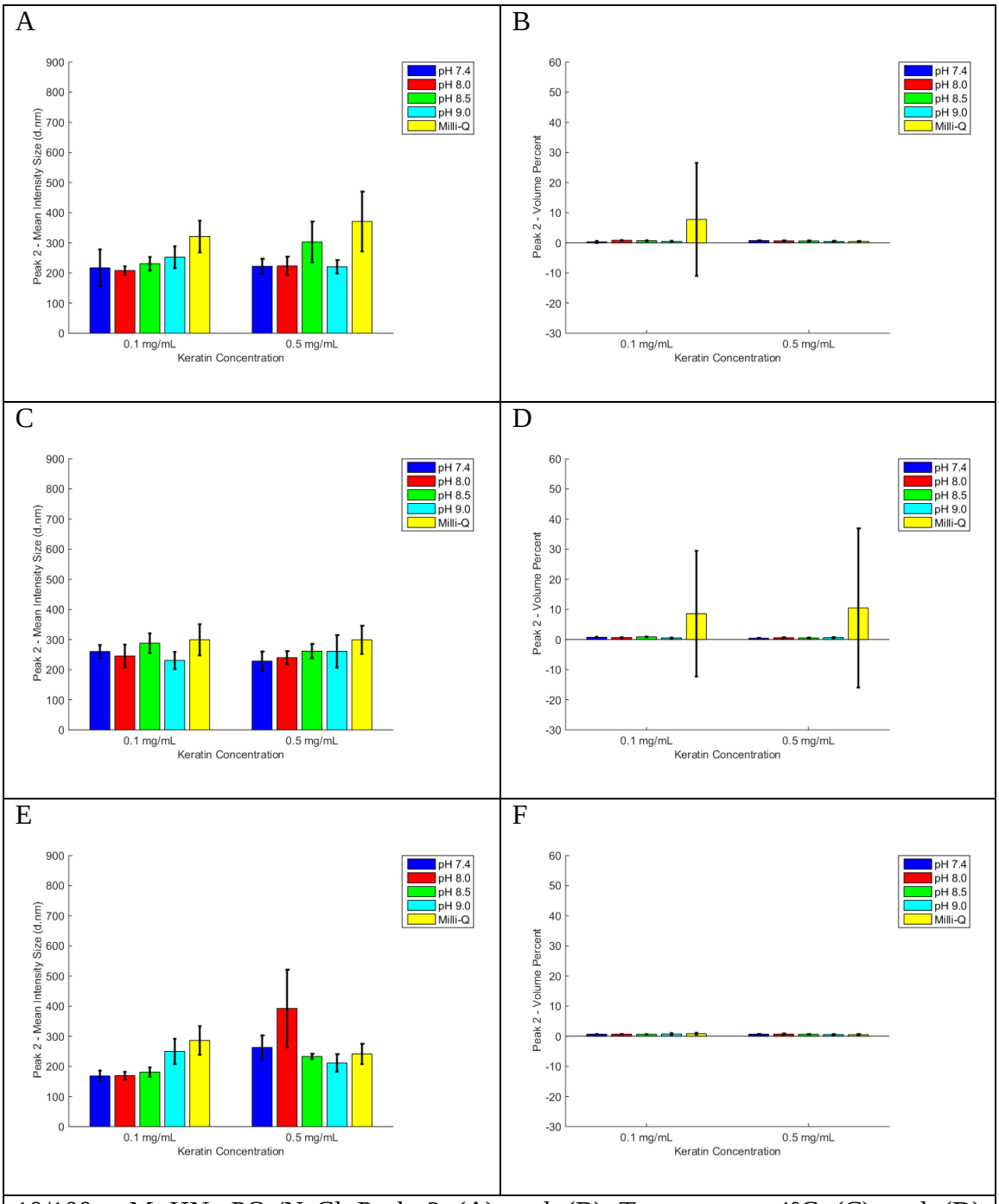

10/100 mM HNa_2PO_4/NaCl Peak 2 (A) and (B) Temperature 4°C (C) and (D) Temperature 25°C (E) and (F) Temperature 37°C

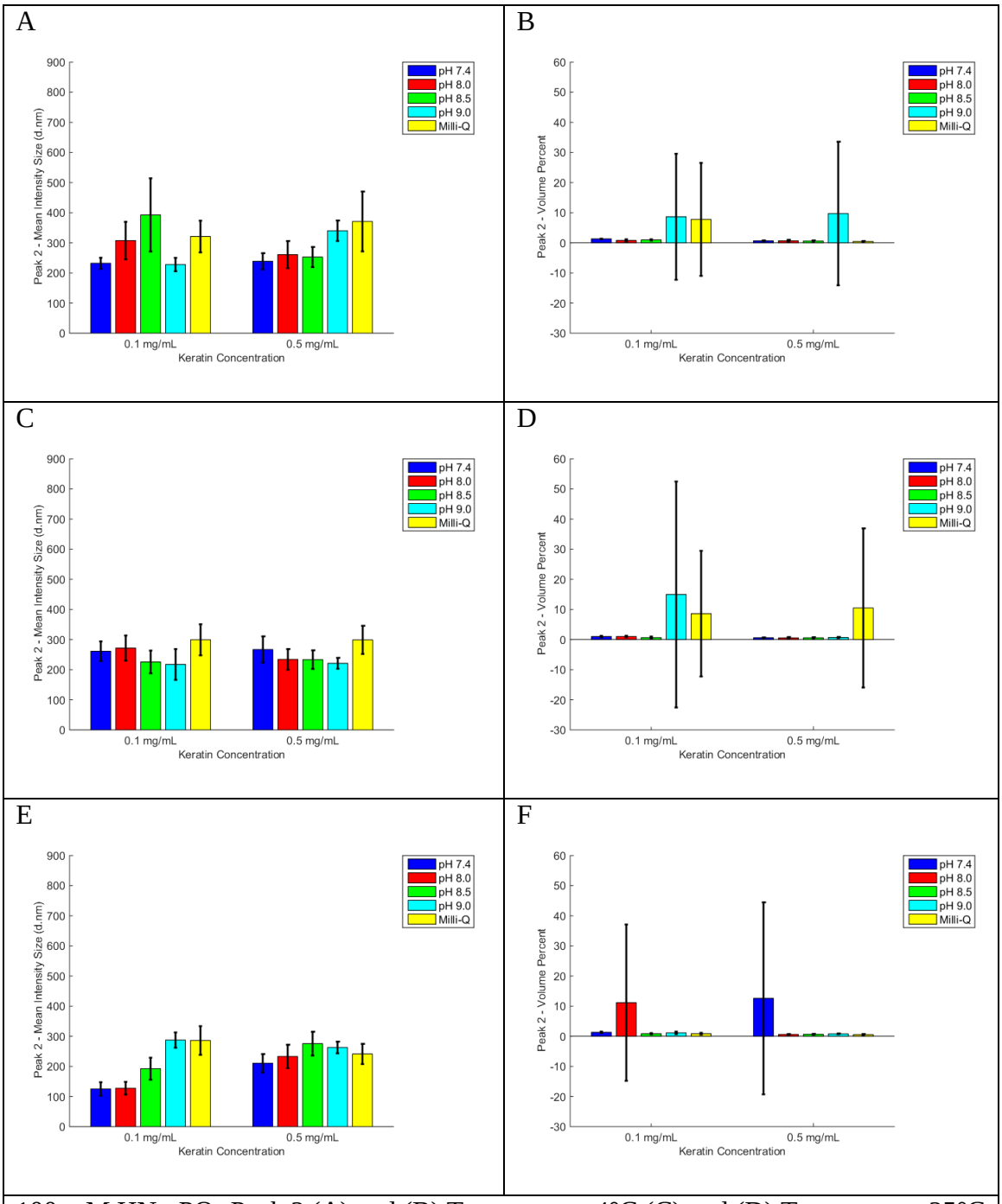

100 mM HNa_2PO_4 Peak 2 (A) and (B) Temperature 4°C (C) and (D) Temperature 25°C (E) and (F) Temperature 37°C

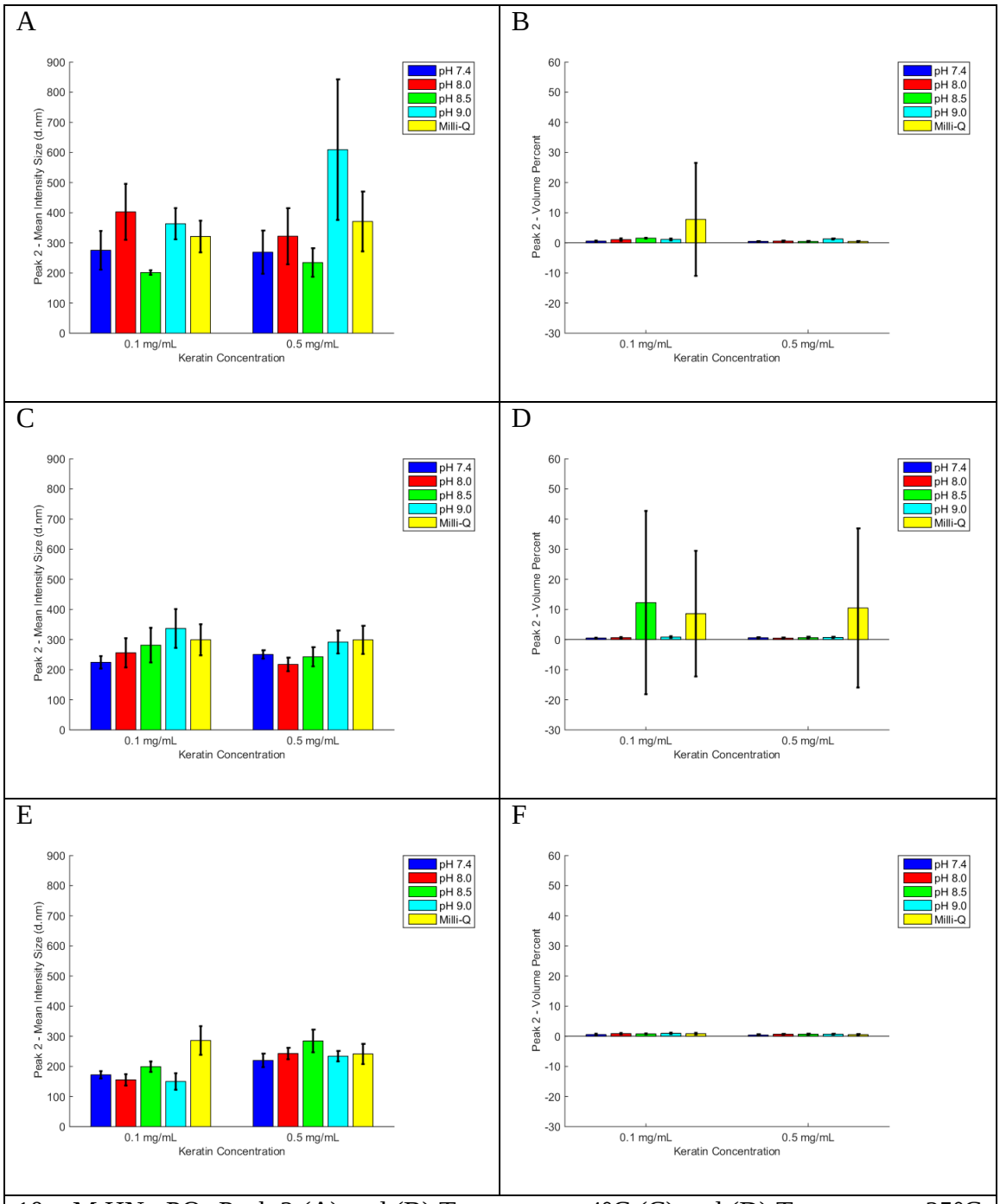

10 mM HNa_2PO_4 Peak 2 (A) and (B) Temperature 4°C (C) and (D) Temperature 25°C (E) and (F) Temperature 37°C